2022 Weather Research and Forecasting (WRF) Modeling Protocol for the LADCO states

Lake Michigan Air Directors Consortium

4415 West Harrison St., Suite 548

Hillside, IL 60162

June 2024

CONTENTS

FIGURES

TABLES

1 Introduction

The Lake Michigan Air Directors Consortium (LADCO) was established by the states of Illinois, Indiana, Michigan, and Wisconsin in 1989. The four states and EPA signed a Memorandum of Agreement (MOA) that initiated the Lake Michigan Ozone Study (LMOS) and identified LADCO as the organization to oversee the study. Additional MOAs were signed by the states in 1991 (to establish the Lake Michigan Ozone Control Program), January 2000 (to broaden LADCO's responsibilities), and June 2004 (to update LADCO's mission and reaffirm the commitment to regional planning). In March 2004, Ohio joined LADCO. Minnesota joined the Consortium in 2012. LADCO consists of a Board of Directors (i.e., the State Air Directors), a technical staff, and various workgroups. The main purposes of LADCO are to provide technical assessments for and assistance to its member states, and to provide a forum for its member states to discuss regional air quality issues.

LADCO is preparing a modeling platform for a 2022 base year to be used in planning modeling for O_3, $PM_{2.5}$, and regional haze (RH). Meteorological inputs are a key component for the LADCO modeling platform. This document is a modeling protocol for the 2022 LADCO meteorological modeling with the Weather Research Forecast Model (WRF). The protocol details the modeling inputs/outputs, modeling procedures, and evaluation procedures that will be used by the LADCO modeling team for meteorology modeling of 2022.

1.1 Organization of the Modeling Protocol

This document presents the LADCO protocol for simulating and evaluating year 2022 meteorology with WRF. The structure and content of this protocol will follow U.S. EPA guidance for the use of models in air quality planning applications. The results from simulations using the WRF modeling configuration proposed here will likely be used as a basis for regulatory air quality modeling by the LADCO states.

This LADCO 2022 WRF Modeling Protocol has the following sections:

1. Introduction: a summary of the background, purpose, objectives of the study, and related modeling studies.
2. Modeling Domain Specifications: the modeling domains selected for the study
3. Modeling Specifications: the modeling software selected for this study and how these models will be applied to simulate 2022 meteorology. This section describes how the meteorological modeling and the WRF model evaluation will be conducted.
4. Meteorological Modeling: the selection of the model configuration, i.e., physics option and parameterization, initialization and other input data, and simulation methodology.
5. Model Performance Evaluation: the procedures for conducting the WRF model performance evaluation.

1.2 Project Participants

Cooperators on the project include Federal agencies and state Departments of Environmental Management. Contributions from Federal agencies include NOAA and U.S. EPA Region 5. The modeling study and model evaluation tasks are conducted by LADCO. Key contacts and their roles in the LADCO 2022 WRF modeling are listed in Table 1-1.

Table 1-1. Key contacts for the LADCO 2022 modeling platform

Name	Role	Organization/Contact
Zac Adelman	QA Manager	Lake Michigan Air Directors Consortium (847) 720-7880 adelman@ladco.org
Tsengel Nergui	LADCO Meteorology Modeler	Lake Michigan Air Directors Consortium (847) 720-7881 nergui@ladco.org
Melissa Sheffer	U.S. EPA Region 5 Advisor	US EPA Region 5 (312) 353-1027 sheffer.melissa@epa.gov
Chris Misenis	EPA WRF Advisor	US EPA OAQPS (919) 541-2046 misenis.chris@epa.gov

1.3 Related Studies

There are numerous meteorological modeling and data analysis studies that are being used to guide the 2022 WRF modeling. The more recent and relevant studies are listed below.

1.3.1 LADCO WRF 2016 Simulation

LADCO used the WRF Advanced Research WRF dynamic core WRF-ARW (Skamarock et al, 2008) to simulate meteorology in the contiguous United States at 12-km resolution and finer grid resolutions in Midwest region for the year 2016. LADCO used WRF Version 4.9.1.1 for 12-km, 4-km, and 1.33-km domains with finer grid resolutions in the Great Lakes Basin and Lake Michigan. The selected physics options for the WRF simulation included the YSU PBL (Hong et al. 2006), Noah LSM (Chen and Dudhia, 2001; Ek et al. 2003), and Thompson microphysics (Thompson et al. 2008, 2016) schemes. The LADCO WRF simulation used 0.25-degree resolution GFS (Grid 4) datasets available from the National Climatic Data Center (NCDC) for initial and boundary conditions and for the four-dimensional data assimilation. The 30-meter resolution land-cover dataset with 40 classes of the 2011 National Land Cover Database (NLCD 2011) was used for all three domains.

LADCO incorporated soil temperature and humidity data from the NASA Short-term Prediction Research and Transition (SPoRT) Center, Land Information System (LIS) into the 4-km WRF simulation and it propagated into the 1.33 km grid modeling. The NASA SPoRT team prepared LIS soil information at 0.03-deg resolution (~3 km) over the continental U.S. to the 4km resolution for our Midwest domain extend for 2016.

LADCO used 1-km sea surface temperature (SST) from the Group for High Resolution Sea Surface Temperatures (GHRSST, Stammer et al., 2003) for the 12-km WRF simulation. A data set of ~1.3 km resolution SST from the Great Lakes Surface Environmental Analysis (GLSEA SST) were used over the Great Lakes in the 4-km and 1.33-km domain simulations. Detailed information on the LADCO WRF 2016 modelling and model performance (LADCO, 2022) can be found at https://www.ladco.org/technical/modeling/ladco-2016-wrf-modeling.

1.3.2 U.S. EPA WRF simulations for 2016, 2017, and 2022

U.S. EPA used version 3.8 of the WRF model, Advanced Research WRF (ARW) core for generating 2016 and 2017 meteorology for photochemical modeling. Selected physics options include Pleim-Xiu land surface model, Asymmetric Convective Model version 2 planetary boundary layer scheme, Kain-Fritsch cumulus parameterization utilizing the moisture-advection trigger (Ma and Tan, 2009), Morrison double moment microphysics, and RRTMG longwave and shortwave radiation schemes (Gilliam and Pleim, 2010). U.S. EPA initialized the 12-km simulation using the 12km North American Model (12NAM) analysis product provided by National Climatic Data Center (NCDC). Analysis nudging for temperature, wind, and moisture was applied above the boundary layer only. The model simulations were conducted continuously. U.S. EPA used the in-house 'ipxwrf' program to initialize deep soil moisture at the start of the run using a 10-day spinup period (Gilliam and Pleim, 2010). Landuse and land cover data were based on the 2011 NLCD. Sea surface temperatures were from the GHRSST dataset.

U.S. EPA assimilated lightning data assimilation from the National Lightning Detection Network (NLDN) to suppress (force) deep convection where lightning is absent (present) in observational data. This method is described by Heath et al. (2016) and was employed to help improve precipitation estimates generated by the model. The model performance details for 2016 (US EPA, 2019) and 2017 (US EPA, 2022) can be found at https://www.epa.gov/sites/default/files/2020-10/documents/met_model_performance-2016_wrf.pdf and https://www.epa.gov/system/files/documents/2022-09/MET_TSD_2017.pdf.

The U.S. EPA WRF 2022 simulation was configured based on model performance sensitivity simulations by the U.S. EPA Office of Research and Development to optimize performance for temperature, mixing ratio, and winds. U.S. EPA used WRF version 4.4.2 to simulate 36- and 12-km domains, initialized directly from 12-km NAM reanalysis and 40-km Eta Data Assimilation System analysis. Selected physics options in the model includes Pleim-Xiu land surface model, Asymmetric Convective Model version 2 planetary boundary layer scheme, Kain-Fritsch cumulus parameterization utilizing the moisture-advection trigger (Ma and Tan, 2009), Morrison double moment microphysics, and RRTMG longwave and shortwave radiation schemes (Gilliam and Pleim, 2010). The model simulations were conducted continuously. U.S. EPA's 'ipxwrf' program was used to initialize deep soil moisture at the start of the run using a 10-day spinup period (Gilliam and Pleim, 2010). The model performance details for the U.S. EPA 2022 simulation (US EPA, 2024) can be found at https://www.epa.gov/system/files/documents/2024-03/wrf_2022_tsd.pdf.

1.3.3 Lake Michigan Ozone Study

The Lake Michigan Ozone Study (LMOS) began in May 2017 as an intensive atmospheric monitoring field campaign along the western shore of Lake Michigan. The LMOS campaign used in-situ surface monitors, aircraft, ships, and satellite data to study the meteorology and chemical drivers of high ground-level ozone concentrations. With the conclusion of the field campaign, LMOS investigators proceeded with a modeling study of the campaign period. They used the data from the field campaign to evaluate different configurations of the WRF model with the objective of finding an optimal configuration for simulating the meteorology conditions that lead to high summer season ozone along the shores of Lake Michigan (Otkin et al., 2023). The LMOS WRF modeling included a Continental US 12-km resolution (CONUS12) domain, a Great Lakes region 4-km domain, and a Lake Michigan 1.33 km domain. Detail on LMOS can be found at: https://www-air.larc.nasa.gov/missions/lmos/. Otkin et al. (2023) conducted a number of WRF simulations for June 2017 to assess the impact of different parameterization schemes, surface datasets, and analysis nudging on lower-tropospheric conditions near Lake Michigan. They compared two parameterization schemes (referred to as AP-XM and YNT, respectively) with various resolution surface datasets including high resolution, real-time datasets for the lake surface temperatures, green vegetation fraction, and soil moisture and temperature from the SPORT LIS. The AP-XM scheme was similar to the EPA's WRF parameterization scheme used for latest WRF simulations. They found that the AP-XM simulation produced more accurate simulation for the 12 km resolution in the Midwest, but that the YNT simulation was superior for higher-resolution nests during the June 2017 period. Additional improvements occurred when using high resolution SST and soil datasets in model simulations.

1.4 Overview of 2022 WRF Modeling Approach

LADCO will apply the WRF meteorological model for the 2022 calendar year using a one-way nested 12/4/1.33-km domain structure. The WRF modeling results for the 2022 annual period will be evaluated against surface and upper-level meteorological observations of wind speed, wind direction, temperature, and humidity. Simulated precipitation fields will be compared against analysis fields from the National Center for Environmental Prediction, NOAA (NCEP) and the Parameter-elevation Relationships on Independent Slopes Model (PRISM) dataset. The 2022 WRF model results will be evaluated against meteorological modeling performance benchmarks and against results from recent regional WRF meteorological modeling studies in the LADCO region.

2 Model Selection

This section discusses the modeling software that LADCO will use to estimate 2022 meteorology fields for the Great Lakes region. The modeling software selection methodology follows U.S. EPA's guidance for regulatory modeling in support of ozone and $PM_{2.5}$ attainment demonstration modeling (US EPA, 2018). EPA recommends that models be selected for regulatory ozone, PM and visibility studies on a "case-by-case" basis with appropriate consideration given to the candidate model's:

- Technical formulation, capabilities and features;
- Pertinent peer-review and performance evaluation history;
- Public availability; and
- Demonstrated success in similar regulatory applications.

All these considerations should be examined for each class of model to be used (e.g., emissions, meteorological, and photochemical) in part because U.S. EPA no longer recommends a specific model or suite of photochemical models for regulatory application as it in the first ozone SIP modeling guidance (US EPA, 1991). Below we identify the most appropriate candidate models for the LADCO 2022 modeling requirements, discuss the candidate model attributes and then justify the model selected using the four criteria above. The science configurations used in this study are introduced in Chapter 3.

2.1 Justification and Overview of Selected Models

The Weather Research Forecast (WRF) model is currently the only prognostic meteorological model that is routinely used in the U.S. in photochemical grid modeling studies. WRF is an open-source model that is developed by the community, with the National Center for Atmospheric Research (NCAR) providing coordination and support. For many years the Mesoscale Meteorology Model version 5 (MM5) was widely used for meteorological research and air quality applications but starting around the year 2000, the WRF model was developed as a technical improvement and replacement to MM5.

WRF meets the following criteria for simulating 2022 meteorology:

- Technical: WRF is based on recent physics and computing techniques, and it is actively supported by NCAR.
- Performance: WRF is being used by thousands of users and has been subjected to a community peer-reviewed development process using the latest algorithms and physics.
- Public Availability: WRF is publicly available and can be downloaded from the WRF website with no costs or restrictions.
- Demonstrated Success: The 2016 LADCO WRF modeling produced meteorology fields that were sufficient for driving air quality model simulations (LADCO, 2022). The U.S. EPA Office of Air Quality Planning and Standards also routinely uses the WRF model for air quality planning modeling.

More details on the selected WRF meteorological model are provided below.

The non-hydrostatic version of the Advanced Research version of the Weather Research Forecast (WRF-ARW[1]) model (Skamarock et al. 2004; 2005; 2006; Michalakes et al. 1998; 2001; 2004) is a three-dimensional, limited-area, primitive equation, prognostic model that has been used widely in regional air quality model applications. The basic model has been under continuous development, improvement, testing and open peer-review for more than two decades and has been used world-wide by hundreds of scientists for a variety of mesoscale studies, including mesoscale convective complexes, urban-scale modeling, air quality studies, frontal weather, lake-effect snows, sea-breezes, orographically induced flows, and operational mesoscale forecasting.

WRF is a next-generation mesoscale prognostic meteorological model routinely used for urban- and regional-scale photochemical, fine particulate, and regional haze regulatory modeling studies. Developed jointly by the National Center for Atmospheric Research and

[1] All references to WRF in this document refer to the WRF-ARW

the National Centers for Environmental Prediction, WRF is maintained and supported as a community model by researchers and practitioners around the globe. The code supports two modes: the Advanced Research WRF (ARW) version and the Non-hydrostatic Mesoscale Model (NMM) version. WRF-ARW is currently the standard model used for regulatory air quality applications in the U.S. It is suitable for use in a broad spectrum of applications across scales ranging from hundreds of meters to thousands of kilometers.

3 Domain Selection

This section presents the model domain definitions for the 2022 WRF simulation, including the domain coverage, resolution, map projection, and nesting schemes for the high-resolution sub-domains.

3.1 Horizontal Modeling Domain

We selected the modeling domains as a trade-off between the need to have high resolution modeling for sources in the Central Midwest versus the ability to perform regional ozone and particulate matter source apportionment modeling among all of the LADCO states. Sharma et al. (2016) indicated that the WRF model with a fine grid spacing of 1-km is capable of accurately yielding the near-surface temperatures and wind speeds associated with the lake breezes over the Chicago area adjoining Lake Michigan. Blaylock et al. (2017) showed that the WRF model with a single 1-km grid domain can capture the fundamental surface wind convergence zones accompanying lake breezes near Great Salt Lake over Utah. Consequently, the LADCO 2022 WRF modeling will use the same 12, 4 and 1.33-km domains as were used in the LADCO 2016 WRF modelling (LADCO, 2022), with the exception of the 1.33-km domain over southeast Michigan and Ohio. The LADCO 2022 WRF simulation will use grids that are based on the standard Lambert Conformal Projection (LCP) used for continental U.S. modeling domains. Table 3-1 includes the specifications for the following domains:

- A 12-km continental U.S. (CONUS) domain that is the same as used by the Multi-Jurisdictional Organizations (MJOs) and other recent modeling studies in the region. The outer domain is defined large enough so that the outer boundaries are far away from our primary areas of interest (i.e., Central Midwest).
- A 4-km Great Lakes regional domain that contains all the LADCO states and portions of adjacent states as well as extending into Canada.
- A 1.33-km Lake Michigan domain that focuses on coastal sites around the lake.

The WRF computational grid was designed so that it can generate photochemical grid model (PGM) meteorological inputs for the nested 12/4/1.33-km domains depicted in Figure 3-1. We defined the WRF modeling domain to be slightly larger than the PGM modeling domains to eliminate the occurrence of boundary artifacts in the meteorological fields used as input to the PGM. Such boundary artifacts can occur as the boundary conditions (BCs) for the meteorological variables come into dynamic imbalance with WRF's atmospheric equations and numerical methods.

Figure 3-1 illustrates the horizontal modeling domains that will be used for the 2022 WRF modeling. The outer 12-km domain (D01) has 472 x 312 grid cells, selected to be consistent with the existing EPA modeling CONUS domain. The projection is Lambert Conformal with the national CONUS grid projection pole of 40°, -97° with true latitudes of 33° and 45°. The 4-km domain (D02) has 445 x 421 grid cells with offsets from the 12-km grid of 223 columns and 116 rows. The 1.33-km domain (D03) has 301 x 493 grid cells with offsets from the 4 km grid of 186 columns and 144 rows.

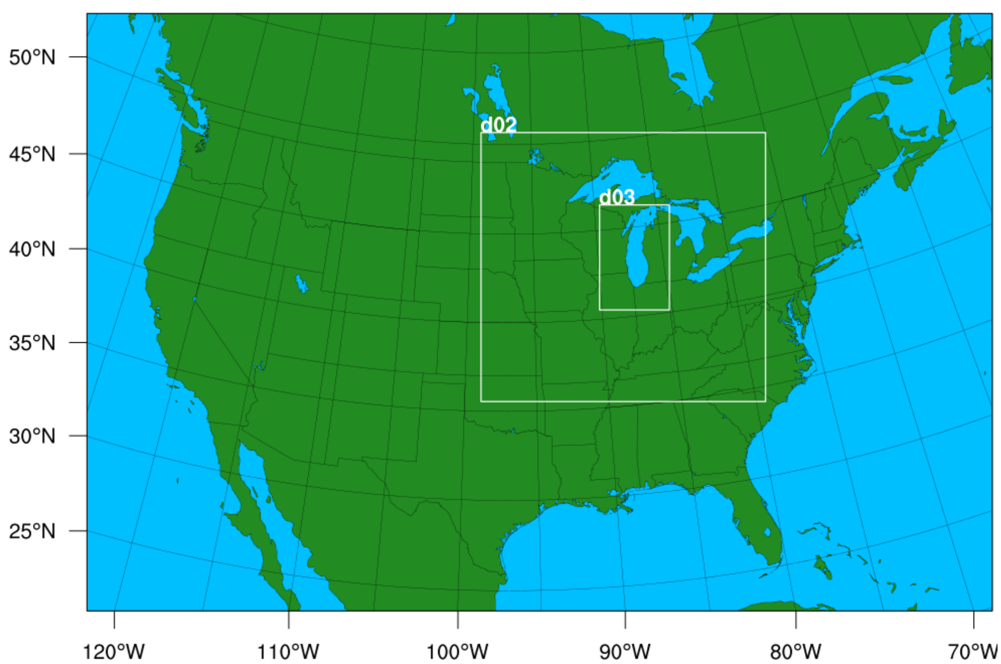

Figure 3-1. WRF 12/4/1.33-km grid structure for the LADCO 2022 meteorological modeling

Table 3-1. Projection parameters for the LADCO 2022 WRF modeling domains

Parameter	Value
Projection	Lambert-Conformal
1st True Latitude	33 degrees N
2nd True Latitude	45 degrees N
Central Longitude	-97 degrees W
Central Latitude	40 degrees N
D01. 12 km X, Y origin offset	-2736 km, -2088 km
D02. 4 km X, Y origin offset	60 km, -696 km
D03. 1.33 km X, Y origin offset	632 km, 712 km

3.2 Vertical Domain Structure

LADCO will run WRF with 36 vertical layer interfaces (35 vertical layers) from the surface up to 50 hPa (~19-km above ground level). The WRF model employs a terrain-following coordinate system defined by pressure, using multiple layers that extend from the surface to the model top. Table 3-2 illustrates the WRF layer structure that we will use for the LADCO 2022 modeling.

Table 3-2. WRF vertical layer specification

WRF Layer	Height (m)	Pressure (Pa)	Sigma	Thickness (m)
36	17,556	5000	0.000	2776
35	14,780	9750	0.050	1958
34	12,822	14500	0.100	1540
33	11,282	19250	0.150	1280
32	10,002	24000	0.200	1101
31	8,901	28750	0.250	969
30	7,932	33500	0.300	868
29	7,064	38250	0.350	789
28	6,275	43000	0.400	722
27	5,553	47750	0.450	668
26	4,885	52500	0.500	621
25	4,264	57250	0.550	581
24	3,683	62000	0.600	547
23	3,136	66750	0.650	517
22	2,619	71500	0.700	393
21	2,226	75300	0.740	285
20	1,941	78150	0.770	276

19	1,665	81000	0.800	180
18	1,485	82900	0.820	177
17	1,308	84800	0.840	174
16	1,134	86700	0.860	170
15	964	88600	0.880	167
14	797	90500	0.900	83
13	714	91450	0.910	82
12	632	92400	0.920	81
11	551	93350	0.930	81
10	470	94300	0.940	80
9	390	95250	0.950	79
8	311	96200	0.960	79
7	232	97150	0.970	78
6	154	98100	0.980	39
5	115	98575	0.985	38
4	77	99050	0.990	39
3	38	99525	0.995	19
2	19	99763	0.9975	19
1	0	100000	1.000	0

4 Meteorological Modeling

This section describes the modeling software configuration and approach that LADCO will use for the 2022 WRF simulation. We present here the WRF test simulation results used for selecting the WRF model configuration and physics options. LADCO will use WRF version 4.5 to simulate the 2022 calendar year using the 12/4/1.33-km domain structure described in Section 3. We will evaluate the WRF modeling results for the 2022 annual period against surface meteorological observations of wind speed, wind direction, temperature and humidity for each domain and compile model performance statistics by month. We will compare the 2022 WRF model performance against meteorological modeling benchmarks and with previous meteorological model performances in the region including LADCO (2022) and U.S. EPA (2019, 2022, 2024). The WRF precipitation fields will be qualitatively assessed against gridded precipitation fields of the NCEP Environmental Modeling Center 4km Gridded Data (GRIB format) Gage-Only Analysis[2] and PRISM datasets form PRISM Climate Group[3].

4.1 Selection of the Model Parameterization and Physics Options

4.1.1 Methods and Discussion

This section documents the WRF version 4.5 model runs and performance evaluations for a series of configurations to optimize the model for simulating weather in the Great Lakes region. LADCO simulated winter (January 1-15) and summer (June 15-30) test cases for which we would evaluate the model performance. We used the results of the test configurations to identify the best configuration for the entire 2022 WRF operational run. We selected the best configuration based on the physical configuration that predicted the key meteorological variables with minimal biases and errors, data output size, the processing time of

[2] Lin, Y., 2006. GCIP/EOP Surface: Precipitation NCEP/EMC 4KM Gridded Data (GRIB) Gage-Only Analysis (GAG) 1996-2001,Version 1.0. UCAR/NCAR - Earth Observing Laboratory. http://data.eol.ucar.edu/dataset/21.048.
[3] PRISM Climate Group (2004), Oregon State Univ. Available at http://prism.oregonstate.edu

initialization and surface observation data, and the WRF model operational run time. Table 4-1 is a list of the nine WRF sensitivity cases used by LADCO to identify the optimal model configuration for simulating 2022 meteorology in the Great Lakes Basin.

Additional details about these nine test cases along with U.S. EPA's two recent 2022 WRF simulations are included in Appendix A. Discussion about these cases, including simulation nomenclature and model performance are included in the rest of this section.

Table 4-1. LADCO WRF sensitivity modeling cases

Simulation ID	Description
WRF45_APX_ERA6_obs	APX physics, ERA5 initialization + data assimilation at 6-hour intervals, surface observational nudging
WRF45_APX_NAM6_obs	APX physics, NAM initialization + data assimilation at 6-hour intervals, surface observational nudging
WRF45_YNT_NAM6_obs	YNT physics, NAM initialization + data assimilation at 6-hour intervals, surface observational nudging
WRF45_APX_NAM_HRRR3	APX physics, NAM initialization + data assimilation at 3-hour intervals, HRRR skin temperature and soil parameter assimilation
WRF45_APX_NAM_HRRR3_obs	APX physics, NAM initialization + data assimilation at 3-hour intervals, HRRR skin temperature and soil parameter assimilation, surface observational nudging
WRF45_YNT_NAM_HRRR3	YNT physics, NAM initialization + data assimilation at 3-hour intervals, HRRR skin temperature and soil parameter assimilation
WRF45_APX_NAM_HRRR6	APX physics, NAM initialization + data assimilation at 6-hour intervals, HRRR skin temperature and soil parameter assimilation
WRF45_APX_NAM_HRRR6_obs	APX physics, NAM initialization + data assimilation at 6-hour intervals, HRRR skin temperature and soil parameter assimilation, surface observational nudging
WRF45_YNT_NAM_HRRR6_obs	YNT physics, NAM initialization + data assimilation at 6-hour intervals, HRRR skin temperature and soil parameter assimilation, surface observational nudging

LADCO's test simulations focused on two sets of physics configurations with various initialization and data assimilation configurations. The YNT physics configuration uses the **Y**SU PBL scheme, Unified **N**oah land surface model (LSM), **T**hompson's microphysics, and

MM5 Monin-Obukhov surface layer option. The YNT configuration was used for the LADCO 2016 WRF simulation and was proven to be the best performing physics option in the Midwest for the summer months (Otkin et al., 2023). The APX physics configuration uses the **A**CM2 PBL scheme, **P**leim-Xiu LSM, **M**orrison 2 moments microphysics, and Pleim-**X**iu surface layer option. The APX physics configuration is based on U.S. EPA's 2016 and 2022 WRF simulations (US EPA, 2019; US EPA, 2024).

Along with the physics configurations, we tested three different reanalysis data sets for initializing the 2022 WRF test cases:

- 31-km resolution the fifth generation of the European Center for Mesoscale Weather Forecast atmospheric reanalysis (ECMWF ERA5) from Copernicus Climate Change Service[4].
- 12 km North American Model (NAM) 218 reanalysis[5] from NOAA.
- 3-km resolution High-Resolution Rapid Refresh (RAPv5/HRRRv4)[6] from NOAA.

We used Global Surface Observation Weather Data collected by the National Centers for Environmental Prediction, NCAR (NCEP)[7] for surface observational nudging in some of the test simulations. Table 4-1 summarizes the combination of physics options, initialization, and nudging configurations that we tested to identify a best-performing WRF configuration for the Great Lakes region.

Figure 4-1 shows the summer and winter period 2-meter air temperature biases for three of the test configurations: WRF45_APX_ERA6_obs, WRF45_APX_NAM6_obs, and WRF45_YNT_NAM6_obs. The WRF45_APX_ERA6_obs configuration overestimated (i.e., warm bias) air temperatures (Average Mean Bias = ~0.5K) across the Midwest for the June test period, while both the WRF45_APX_NAM6_obs and the WRF45_YNT_NAM6_obs

[4] https://cds.climate.copernicus.eu/
[55] https://www.ncei.noaa.gov/thredds/catalog/model-namanl/
[6] https://noaa-hrrr-bdp-pds.s3.amazonaws.com/hrrr
[7] https://data.rda.ucar.edu/ds461.0

configurations underestimated (i.e., cool bias) the observed temperatures on average by about -0.2 K. The configurations using the APX physics had higher average Root Mean Square Errors (RMSE = 1.9-2.0 K) relative to the simulation that used YNT physics (RMSE =1.58 K).

While the WRF45_YNT_NAM6_obs configuration had the best overall temperature performance for June, it had a notable cool bias in January of about -0.6 K. The winter cool bias was more pronounced in MN, WI, and parts of MI. The configurations using APX physics did not have the systematic cold bias as the YNT configuration and overall showed better skill at predicting temperatures for the winter test period. Furthermore, the WRF45_YNT_NAM6_obs simulation for January had positive wind speed biases (MB = 0.5 m/s) in MN, WI and MI due to the temperature underestimation in these parts of the domain (not shown).

Figure 4-1. June (top row) and January (bottom row) average test period 2-m temperature mean bias for the 4-km resolution Midwest domain WRF simulations.

	WRF45_APX_ERA6_obs	**WRF45_APX_NAM6_obs**	**WRF45_YNT_NAM6_obs**
June	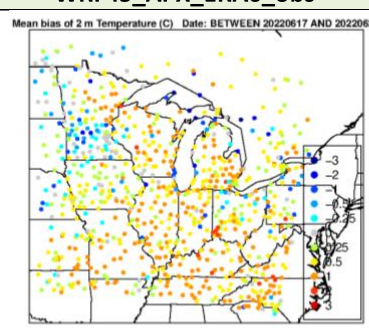 **RMSE = 1.94 K; MB = 0.52 K**	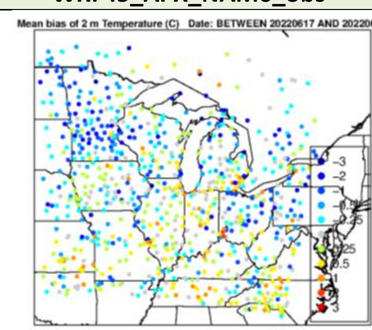 **RMSE = 2.02 K; MB = -0.19 K**	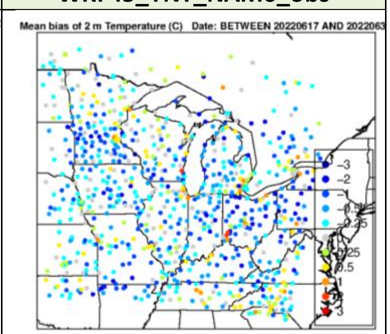 **RMSE = 1.58 K; MB = -0.21 K**
January	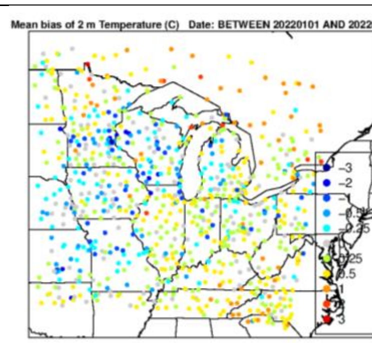 **RMSE = 1.87 K; MB = 0.23 K**	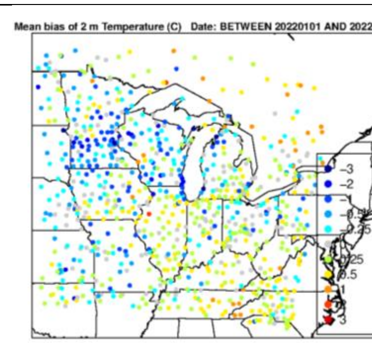 **RMSE = 1.96 K; MB = 0.00 K**	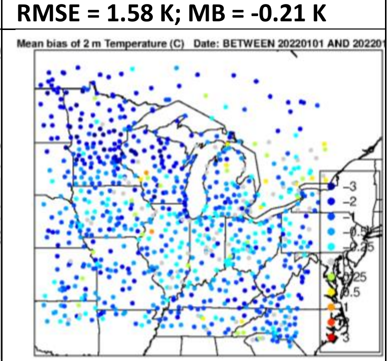 **RMSE = 1.85 K; MB = -0.62 K**

Otkin et al. (2023) and LADCO (2022) demonstrated that assimilation of high-resolution sea surface temperature (SST) and soil condition data into a WRF simulation adds value for predicting air quality-relevant conditions in the Great Lakes region. Lake breeze dynamics play an important role in warm season surface ozone concentrations near the lake shore in the Midwest. The model performance for the lake-to-land and land-to-lake circulations is strongly dependent upon the accuracy of the SST over the Great Lakes and the soil conditions (temperature and moisture) near the lakeshore. As the NASA SpORT LIS data like those used for the LADCO 2016 WRF simulation are not available for 2022 we sought other soil data to assimilate into our 2022 simulation.

Figure 4-2 shows the comparison of the SST over the Great Lakes and skin temperature over the rest of the Midwest domain from the 12-km resolution NAM and the 3-km resolution HRRRv4 reanalysis data. As the finer resolution HRRRv4 reanalysis provides more spatially resolved features to support better simulations of the lake breeze dynamics, we experimented with these data to understand if they add value to the LADCO 2022 WRF modeling.

Figure 4-2. Skin Temperature calculated from the 12-km NAM and 3-km HRRRv4 Reanalysis at 12:00 UTC (top) and 18:00 UTC (bottom) on June 16, 2022

Skin Temperature from the 12-km NAM	Skin Temperature from the 3-km HRRRv4
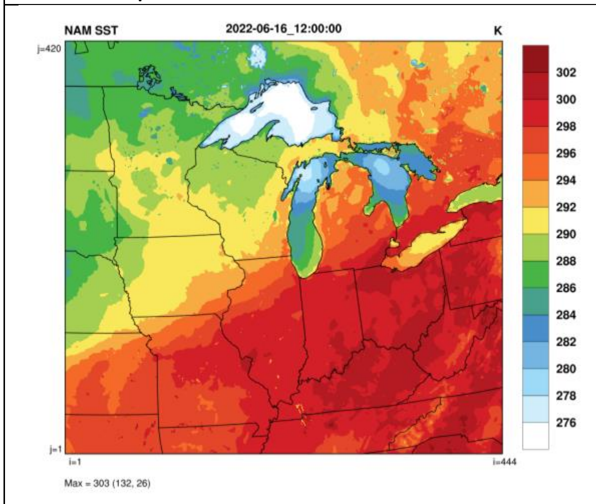	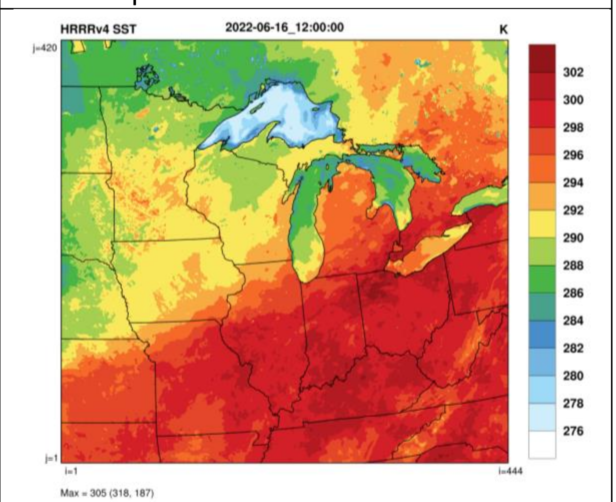

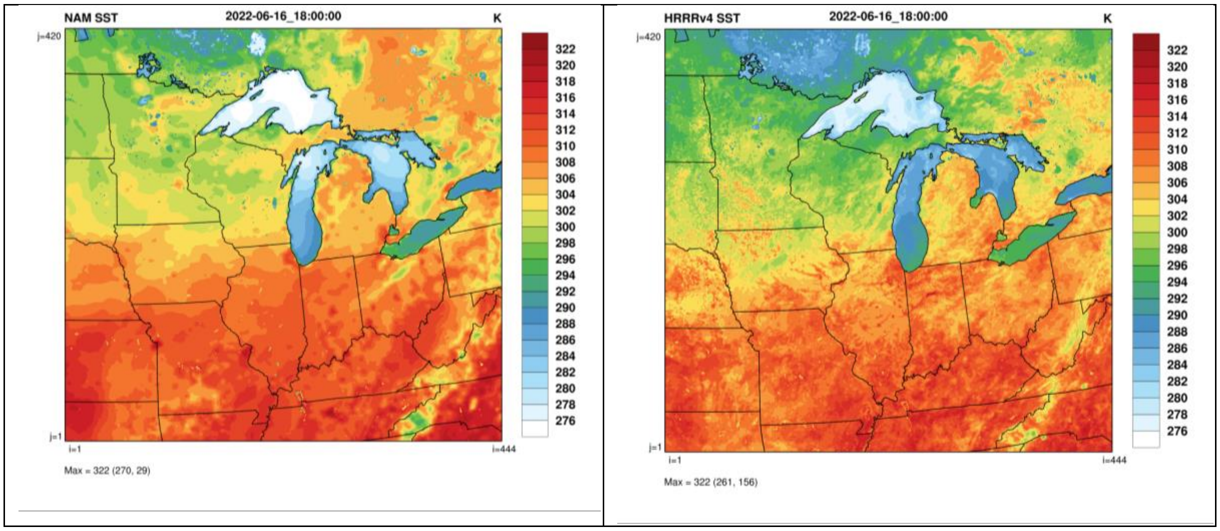

LADCO modified the base WRF45 APX_NAM6_obs and WRF45 YNT_NAM6_obs configurations by using forcing data (i.e., initialization and FDDA) that were a hybrid of the 12-km NAM and 3-km HRRRv4 reanalysis data. We experimented with assimilating the forcing data using grid nudging at a higher frequency (3-hour vs 6-hour intervals) to strengthen the influence of the HRRR SST and soil parameters on the WRF forecast. The June and January 2-meter air temperature biases for a subset of these tests are shown in Figure 4-3.

The use of the blended NAM and HRRRv4 in the APX configuration generally lowered the temperature predictions in both test periods, which had a performance benefit to the base configuration for areas of the domain with a warm bias, but a disbenefit to areas with a cold bias. Due to the heterogeneity in the temperature biases across the Midwest domain, we consider the domain averaged RMSE a better metric of model performance because it is not as subject to compensating, intra-domain signals as domain averaged mean bias. The hybrid forcing simulation without observational nudging resulted in increased RMSEs in both test periods relative to the base configuration (not shown), indicating the importance of using surface observational data assimilation for retrospective WRF modeling. When the hybrid forcing simulation is combined with surface observation grid nudging, we achieved the best performance (RMSE=~1.6K and low mean bias) for both June and January test periods. There was not a substantial difference in the hybrid forcing simulations between the 3-hour and 6-hour assimilation frequencies. Given the additional processing times and data sizes required to support the more frequent assimilation configuration, we will use the 6-hour assimilation approach for our operational WRF simulations for 2022.

Additional model performance plots comparing the WRF45_YNT_NAM_HRRR6_obs and WRF45_APX_NAM_HRRR6_obs simulations for winter/summer RMSE and mean bias for temperature, mixing ratio, and winds are provided in Appendix C.

Figure 4-3. June (top row) and January (bottom row) average test period 2-m temperature mean bias for the experiments using 3-hr interval blended NAM-HRRR reanalysis (middle column) and 6-hr interval reanalysis (right column).

	WRF45_APX_NAM6_obs	LADCO_2022_APX_NAM-HRRR3_obs	LADCO_2022_ APX_NAM-HRRR6_obs
June	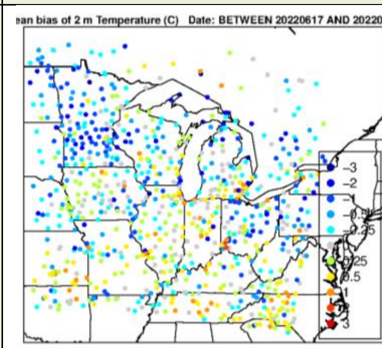 **RMSE = 2.02 K; MB = -0.19 K**	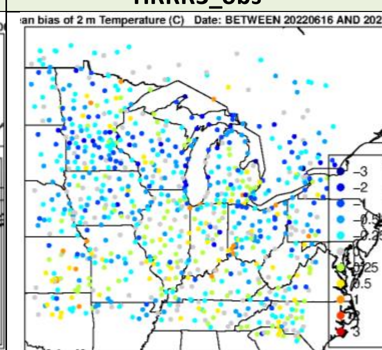 **RMSE = 1.62 K; MB = -0.10 K**	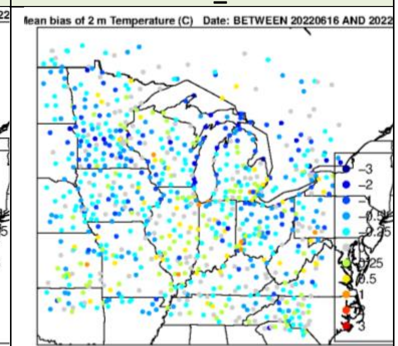 **RMSE = 1.61 K; MB = -0.06 K**
January	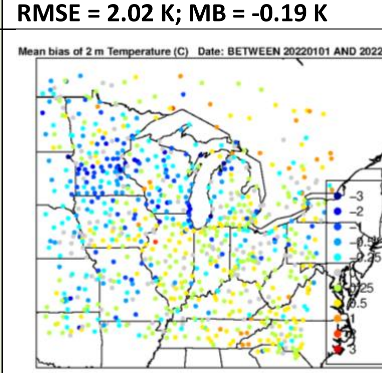 **RMSE = 1.96 K; MB = 0.00 K**	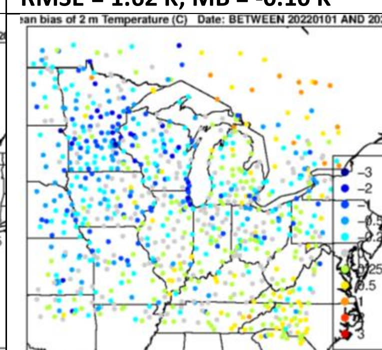 **RMSE = 1.66 K; MB = 0.01 K**	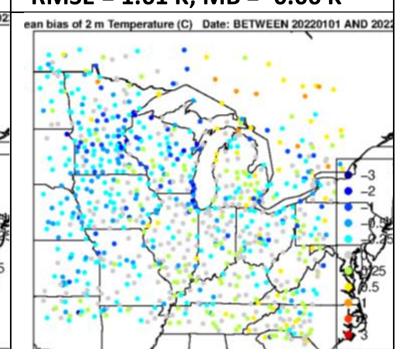 **RMSE = 1.54 K; MB = -0.02 K**

4.1.2 Summary and Configuration Selection

Table 4-2 and Table 4-3 show for the nine LADCO configuration sensitivities the WRF 4-km domain average root mean square error (RMSE) values for the June and January test periods, respectively. Table 4-4 and Table 4-5 show for the nine LADCO configuration sensitivities the

WRF 4-km domain average bias values for the June and January test periods, respectively. The major conclusions from these sensitivities are:

- Although the simulation initialized and forced with ERA5 had domain average RMSE values that are in the range of the other simulations, there are areas of significant bias within the 4-km domain that invalidates this configuration
- For the summer period, the WRF45_YNT_NAM6_obs, WRF45_APX_NAM_HRRR6_obs, and WRF45_YNT_HRRR6_obs simulations had similar performance and generally outperformed the rest of the configurations
- For the winter period, the WRF45_APX_NAM_HRRR3_obs and WRF45_APX_NAM_HRRR6_obs simulations had similar performance and generally outperformed the rest of the configurations

Given that the configurations that used YNT physics did not simulate the winter period well, and based on the results of these configuration experiments, LADCO will use the WRF45_APX_NAM_HRRR6_obs configurations to simulate 2022 meteorology fields to support air quality model applications for the Great Lakes region. This configuration offers the best combination of model performance across the two test periods, and computational and data processing efficiency. Complete details of the model and operational configurations for this configuration are included in the following section.

Table 4-2. LADCO 4-km WRF sensitivity simulation root mean square error for June 2022 test cases; green shading indicates best performing case for each variable

Simulation ID	2m Temp	2m Mixing Ratio	10m WS	10m WD
WRF45_APX_ERA6_obs	1.94	1.90	1.40	34.30
WRF45_APX_NAM6_obs	2.02	1.79	1.37	33.31
WRF45_YNT_NAM6_obs	1.58	1.54	1.43	33.24
WRF45_APX_NAM_HRRR3	1.87	1.74	1.48	36.03
WRF45_APX_NAM_HRRR3_obs	1.62	1.68	1.39	33.38
WRF45_YNT_NAM_HRRR3	2.00	1.69	1.57	36.21
WRF45_APX_NAM_HRRR6	2.40	4.26	1.40	35.56
WRF45_APX_NAM_HRRR6_obs	1.61	1.64	1.39	34.09
WRF45_YNT_NAM_HRRR6_obs	1.55	1.54	1.43	33.88

Table 4-3. LADCO 4-km WRF sensitivity simulation root mean square error for January 2022 test cases; green shading indicates best performing case for each variable

Simulation ID	2m Temp	2m Mixing Ratio	10m WS	10m WD
WRF45_APX_ERA6_obs	1.87	0.45	1.47	25.04
WRF45_APX_NAM6_obs	1.96	0.46	1.45	24.66
WRF45_YNT_NAM6_obs	1.85	0.40	1.63	24.95
WRF45_APX_NAM_HRRR3	2.53	0.54	1.55	27.28
WRF45_APX_NAM_HRRR3_obs	1.66	0.48	1.47	24.22
WRF45_YNT_NAM_HRRR3	N/A	N/A	N/A	N/A
WRF45_APX_NAM_HRRR6	2.04	0.50	1.52	26.13
WRF45_APX_NAM_HRRR6_obs	1.54	0.42	1.46	24.35
WRF45_YNT_NAM_HRRR6_obs	1.90	0.40	1.63	24.82

Table 4-4. LADCO 4-km WRF sensitivity simulation mean bias for June 2022 test cases; green shading indicates best performing case for each variable

Simulation ID	2m Temp	2m Mixing Ratio	10m WS	10m WD
WRF45_APX_ERA6_obs	0.52	-0.71	0.06	3.37
WRF45_APX_NAM6_obs	-0.19	-0.42	-0.01	2.33
WRF45_YNT_NAM6_obs	-0.21	0.15	0.09	2.18
WRF45_APX_NAM_HRRR3	-0.06	-0.03	0.27	6.45
WRF45_APX_NAM_HRRR3_obs	-0.10	0.14	0.14	3.87
WRF45_YNT_NAM_HRRR3	-0.22	-0.23	0.43	5.95
WRF45_APX_NAM_HRRR6	-0.48	-3.64	0.00	2.14
WRF45_APX_NAM_HRRR6_obs	-0.06	0.41	-0.10	2.36
WRF45_YNT_NAM_HRRR6_obs	-0.26	0.12	0.10	2.11

Table 4-5. LADCO 4-km WRF sensitivity simulation mean bias for January 2022 test cases; green shading indicates best performing case for each variable

Simulation ID	2m Temp	2m Mixing Ratio	10m WS	10m WD
WRF45_APX_ERA6_obs	0.23	0.16	0.20	4.68
WRF45_APX_NAM6_obs	0.00	0.17	0.12	4.19
WRF45_YNT_NAM6_obs	-0.62	0.00	0.50	3.44
WRF45_APX_NAM_HRRR3	0.07	0.20	0.17	7.11
WRF45_APX_NAM_HRRR3_obs	0.01	0.18	0.20	5.18
WRF45_YNT_NAM_HRRR3	N/A	N/A	N/A	N/A
WRF45_APX_NAM_HRRR6	0.05	0.19	0.12	6.10
WRF45_APX_NAM_HRRR6_obs	-0.02	0.14	-0.13	4.02
WRF45_YNT_NAM_HRRR6_obs	-0.78	-0.01	0.50	3.54

4.2 Model Version Selection and Application

LADCO will use WRF version 4.5 to simulate meteorology in 2022 using the WRF45_APX_NAM_HRRR6_obs configuration described in the previous section. The WRF preprocessor programs GEOGRID, UNGRIB, and METGRID will be used to create model inputs. The 2022 WRF simulated meteorological fields will be used to support emissions and photochemical modeling in support of air quality planning and State Implementation Plans for our member states.

4.3 Topographic Inputs

The WRF test runs discussed in Section 4.1 used topographic data from the National Land Cover Database 2011 dataset (NLCD 2011). Topographic information for the 2022 WRF will be developed using the National Land Cover Database 2011 Update available from the National Center for Atmospheric Research (NCAR) based on the 9 sec (~300 m) data[8].

4.4 Vegetation Type and Land Use Inputs

We will use 2019 National Landcover Data (NLCD 2019) for the vegetation and land use inputs to WRF. The NLCD is a 40-category, 30-meter resolution dataset of land-cover for the continental U.S. The WRF-compatible version of the NLCD is supplemented with the MODIS 20-category land cover data for regions outside of the U.S.

Table 4-6 lists the NLCD and MODIS landcover categories that will be available for this simulation.

Table 4-6. NLCD and MODIS landuse categories for the 2022 WRF modeling

MODIS		**NLCD**	
Number	**Category Name**	**Number**	**Category Name**
1	Evergreen Needleleaf Forest	22	Perennial Ice/Snow
2	Evergreen Broadleaf Forest	23	Developed Open Space
3	Deciduous Needleleaf Forest	24	Developed Low Intensity

[8] https://www.mrlc.gov/nlcd2019.php

4	Deciduous Broadleaf Forest
5	Mixed Forests
6	Closed Shrublands
7	Open Shrublands
8	Woody Savannas
9	Savannas
10	Grasslands
11	Permanent Wetlands
12	Croplands
13	Urban And Built Up
14	Cropland/Natural Vegetation Mosaic
15	Permanent Snow and Ice
16	Barren or Sparsely Vegetated
17	IGBP Water
25	Developed Medium Intensity
26	Developed High Intensity
27	Barren Land (Rock/Sand/Clay)
28	Deciduous Forest
29	Evergreen Forest
30	Mixed Forest
32	Shrub/Scrub
33	Grassland/Herbaceous
37	Pasture/Hay
38	Cultivated Crops
39	Woody Wetlands
40	Emergent Herbaceous Wetlands

4.5 Atmospheric Data Inputs

The LADCO WRF simulation for 2022 will be initialized with a blend of the 12-km (Grid #218) North American Model (NAM) [9] and the 3-km resolution High-Resolution Rapid Refresh (RAPv5/HRRRv4) [10] available from NOAA National Centers for Environmental Information (NCEI) server. The Global Surface Observation Weather Data collected by the National Centers for Environmental Prediction, NCAR (NCEP)[11] will be used for the surface observation grid nudging.

4.6 Time Integration

Third order Runge-Kutta integration will be used (rk_ord = 3). The maximum time step, defined for the outer-most domain (12 km) only, should be set by evaluating the following equation:

[9] https://www.ncei.noaa.gov/thredds/catalog/model-namanl/
[10] https://noaa-hrrr-bdp-pds.s3.amazonaws.com/hrrr
[11] https://data.rda.ucar.edu/ds461.0

$$dt = \frac{6dx}{F_{map}}$$

Where *dx* is the grid cell size in km, F_{map} is the maximum map factor (which can be found in the output from the WRF program REAL.EXE), and *dt* is the resulting time-step in seconds. For the case of the 12-km domain, *dx* = 12 and F_{map} = 1.08, so *dt* should be taken to be less than 200 seconds. Longer time steps typically lead to Courant-Friedrichs-Lewy (CFL) condition errors, associated with large vertical velocity values, which tend to occur in areas of steep terrain, especially during very stable conditions in winter. For the 2022 modeling, we will use a fixed time step of 60 seconds for 12km grid domain, 20 seconds for 4km grid domain, and 6.67 seconds for 1.33 km grid domain.

4.7 Diffusion Options

Horizontal Smagorinsky first-order closure (km_opt = 4) with sixth-order numerical diffusion (diff_6th_opt = 2) will be used.

4.8 Lateral Boundary Conditions

Lateral boundary conditions will be specified from the initialization dataset on the 12-km domain with continuous updates nested from the 12-km domain to the 4-km domain and from the 4-km domain to the 1.3-km domain, using one-way nesting (feedback = 0).

4.9 Top and Bottom Boundary Conditions

The no damping option will be selected for the top boundary condition and consistent with the model application for non-idealized cases, the bottom boundary condition will be selected as physical, not free-slip.

4.10 Sea Surface Temperature Inputs

The 3-hr interval HRRRv4 data inherently provides finer resolution skin temperature in the CONUS domain including high-resolution sea surface temperature (SST) over the Great

Lakes, which is important for simulating the lake breeze dynamics in our 4-km Midwest and the 1.3-km Lake Michigan domains.

4.11 FDDA Data Assimilation

The WRF model will be run with analysis nudging using Four-Dimensional Data Assimilation (FDDA) for the 12-km and 4-km domains only. FDDA will not be used for the 1.33-km domain due to limited observations available over Lake Michigan. We will use analysis nudging coefficients up to $3x10^{-4}$ s^{-1} for horizontal wind and temperature and analysis nudging coefficients up to $1.0x10^{-5}$ s^{-1} for water vapor mixing ratio, depending on domain. Only aloft nudging will be performed; no nudging will be applied for wind, temperature, and mixing ratio in the planetary boundary layer (Otte et al., 2008)[12].

4.12 WRF Physics Options

LADCO selected WRF physics options for the 2022 WRF simulation based on the best performing configurations among the series of sensitivity runs described in Section 4.1. Table 4-7 lists the physics options that LADCO will use to simulate ozone season and non-ozone season meteorology for 2022.

Table 4-8 provides additional details about the LADCO 2022 WRF configurations and compares them to other recent WRF simulations that were evaluated for the Great Lakes region.

Table 4-7. Options proposed for the LADCO 2022 WRF modeling

WRF Treatment	Option
Microphysics	Morrison 2 moment (mp_physics = 10)
Longwave Radiation	RRTMG (ra_lw_phsysics = 4)
Shortwave Radiation	RRTMG (ra_sw_phsysics = 4)

[12] Otte, T.L. (2008). The impact of nudging in the meteorological model for retrospective air quality simulations. Part II: Evaluating collocated meteorological and air quality observations. Journal of Applied Meteorology and Climatology, 47(7): 1868-1887.

WRF Treatment	Option
Land Surface Model (LSM)	Pleim-Xiu (sf_surface_physics=7)
Planetary Boundary Layer (PBL) scheme	ACM2 (bl_pbl_physics=7)
Cumulus parameterization	Kain-Fritsch in the 12-km and 4-km domains with the moisture-advection based trigger; no cumulus parameterization in the 1.33 km domain (cu_physics=1; trigger option =2)
Analysis nudging	Nudging applied to winds, temperature and moisture in the 12-km and 4-km domains above the PBL
Initialization Dataset	Blend of NAM218 (12-km) and HRRRv4 (3-km), 6-hr interval
Surface OBSGRID nudging	Surface observational data from the NCAR Research Data Archive (RSA)

Table 4-8. Comparison of the LADCO 2022 WRF configuration to recent configurations for modeling in the LADCO region

WRF Treatment	LADCO 2022	LADCO 2016	EPA 2016	EPA 2022
Diffusion	Horizontal Smagorinsky first-order closure			
Microphysics	Morrison 2 moments	Thompson	Morrison 2 moments	Morrison 2 moments
LW Radiation	RRTMG			
SW Radiation	RRTMG			
LSM	Pleim-Xiu	Noah	Pleim-Xiu	Pleim-Xiu
PBL scheme	ACM2	YSU	ACM2	ACM2
Cumulus clouds	Kain-Fritsch in the 12-km and 4-km domains. None in the 1.3-km domain.		Kain-Fritsch with moisture-advection trigger	
Analysis nudging	uv, t, q in the 12-km and 4-km domains		uv, t, q in the 12-km domain	
Analysis Nudging Coefficients	uv: 0.0003 (d01), 0.0001 (d02), t: 0.0003 (d01), 0.0001(d02), q: 0.00001			
PBL Analysis Nudging	None			
Surface Obs Nudging	Yes for 12-km and 4-km domains		Yes	
ICBC	A blend of 12-km NAM and the 3-hr HRRRv4	12-km NAM	12-km NAM	12-km NAM and 40-km EDAS analysis

WRF Treatment	LADCO 2022	LADCO 2016	EPA 2016	EPA 2022
				where applicable
LULC	NLCD 2019	NLCD 2011	NLCD 2011	NLCD 2011
NLDN Lightning	No	No	Yes	Yes
Soil data assimilation	3-hr HRRRv4	NASA SpORT LIS	No	No

4.13 WRF Output Variables

The WRF model will be configured to output additional variables to support air quality modeling with the Comprehensive Air Quality Model with Extensions (CAMx) and the Community Multiscale Air Quality Model (CMAQ). The following fields will be activated in the WRF output history files:

- Fractional land use (LANDUSEF)
- Aerodynamic resistance (RA)
- Stomatal resistance (RS)
- Vegetation fraction in the Pleim-Xiu LSM (VEGF_PX)
- Roughness length (ZNT)
- Inverse Monin-Obukhov length (RMOL).

4.14 WRF Simulation Methodology

As described above, LADCO selected the WRF45_APX_NAM_HRRR6_obs configuration for simulating 2022 meteorology for air quality modeling applications in the Great Lakes region. To enable a faster turn-around of the simulations LADCO will run multiple periods simultaneously using the Amazon Web Services (AWS) compute cloud. We will run WRF in 3-month blocks using a 5-day initialization period with a 60-second integration time step. Model results will be output every 60 minutes and each output file will include 24-hours of data.

LADCO will run the model at 12-km, 4-km, and 1.33-km grid resolution from December 20, 2021 through February 1, 2023 using one-way grid nesting (i.e., the meteorological conditions are allowed to propagate from the coarser grid to the finer grid, but not vice versa). The namelist files for the WPS and WRF-ARW configurations that will be used for this study are included in Appendix B.

4.15 Evaluation Approach

LADCO will use a combination of qualitative and quantitative metrics to assess the performance of the 2022 WRF modeling. The quantitative analysis will be divided into monthly summaries of 2-m temperature, 2-m water vapor mixing ratio, and 10-m wind speed and direction using the boreal seasons to help generalize the model bias and error relative to a standard performance benchmark. The evaluation will focus on the 12-km and 4-km domains in the LADCO states and supplemented with select diurnal and time series analyses. Additional analysis will include a qualitative evaluation of the WRF daily and monthly precipitation fields against NCEP and PRISM fields. The National Oceanic and Atmospheric Administration (NOAA) Earth System Research Laboratory (ESRL) Meteorological Assimilation Data Ingest System (MADIS) will be used to evaluate the winds, temperatures, and water vapor mixing ratios in this simulation.

Calculating bulk statistics over a continental or regional scale domain is problematic because compensating errors and biases get averaged out when evaluating model performance across a broad spectrum of physical and dynamical conditions. Evaluation across large spatial and temporal scales masks important sub-regional, local, and episodic features in the meteorology. Despite these issues, cursory statistics of domain wide, seasonal and monthly model performance provide a high-level overview of WRF’s ability to simulate meteorology conditions in the region. We will augment the 12/4/1.33-km domain-wide analysis with statistics by state. Particular attention will be paid to the model performance in the LADCO states.

Additional details of how we will conduct the model performance evaluation for this simulation are provided in Section 5.

4.16 Reporting

The 2022 WRF simulation and evaluation will be documented in a final report and through site-specific performance plots.

5 Meteorological Model Performance Evaluation

LADCO will evaluate our 2022 WRF modeling using a combination of qualitative and quantitative metrics. The quantitative approach calculates model performance statistics using predicted and observed surface meteorological variables. We will compare the performance statistics for the 2022 WRF simulation with published performance benchmarks. The qualitative approach compares the spatial distribution of the model-estimated precipitation with precipitation fields from the NCEP and PRISM[13] precipitation analysis fields based on observations using graphical outputs, and a comparison of the WRF estimated cloud cover with satellite observations.

5.1 QUANTITATIVE EVALUATION USING SURFACE METEOROLOGICAL OBSERVATIONS

LADCO will use a statistical evaluation approach with the model bias and error for surface wind speed, wind direction, temperature, and water vapor mixing ratio. We will compare the 2022 WRF performance statistics to benchmarks developed based on a history of meteorological modeling as well as past meteorological model performance.[14] Model performance will be evaluated at each meteorological station within the 12-km CONUS and 4-km LADCO modeling domains. The model performance statistics will also be averaged for each LADCO state.

MADIS is the observed database for winds, temperature, and water mixing ratio that will be used to evaluate WRF for this study.

[13] http://www.prism.oregonstate.edu/

[14] Emery, C., E. Tai, and G. Yarwood, 2001. Enhanced Meteorological Modeling and Performance Evaluation for Two Texas Ozone Episodes. Prepared for the Texas Natural Resource Conservation Commission, prepared by ENVIRON International Corporation, Novato, CA. 31 August. (http://www.tceq.texas.gov/assets/public/implementation/air/am/contracts/reports/mm/EnhancedMetModelingAndPerformanceEvaluation.pdf).

The quantitative model performance evaluation of WRF using surface meteorological measurements will be performed using the publicly available Atmospheric Model Evaluation Tool (AMET)[15] evaluation tools. These tools calculate statistical performance metrics for bias, error, and correlation for surface winds, temperature, and mixing ratio and can produce time series of predicted and observed meteorological variables and performance statistics.

A full annual model evaluation is very difficult to summarize in a single document, especially a simulation that could be used for many different purposes. Thus, the WRF model evaluation report will present results for several sub-regions, even at the individual site level within the 4-km domain, leaving potential data users to independently judge the adequacy of the model simulation. Model performance statistics will be aggregated by month, for high pollution days, and lake-breeze days. Overall comparisons are offered to judge the model's efficacy, but this review does not necessarily cover all potential user needs and applications.

Statistical metrics will be presented for each LADCO state and for the U.S. portion of the 12-km and 4-km modeling domains. To evaluate the performance of the WRF 2022 simulation for the U.S., a number of performance benchmarks for comparison will be used. Emery et al. derived and proposed a set of daily performance "benchmarks" for typical meteorological model performance.[16] These standards were based upon the evaluation of about 30 MM5 and RAMS meteorological simulations of limited duration (multi-day episodes) in support of air quality modeling study applications performed over several years. The simulations were ozone model applications for cities in the Eastern and Midwestern U.S. and Texas that were primarily simple (flat) terrain and simple (stationary high pressure causing stagnation) meteorological conditions. More recently, these benchmarks have been used in annual meteorological modeling studies that include areas with complex terrain and more

[15] http://www.cmascenter.org

[16] Emery, C., E. Tai, and G. Yarwood, 2001. "Enhanced Meteorological Modeling and Performance Evaluation for Two Texas Ozone Episodes." Prepared for the Texas Natural Resource Conservation Commission, prepared by ENVIRON International Corporation, Novato, CA. 31-August. http://www.tceq.texas.gov/assets/public/implementation/air/am/contracts/reports/mm/EnhancedMetModelingAndPerformanceEvaluation.pdf

complicated meteorological conditions; therefore, they must be viewed as being applied as *guidelines* and not *bright-line* numbers. That is, the purpose of these benchmarks is not to give a passing or failing grade to any one particular meteorological model application, but rather to put its results in context with other model applications and meteorological data sets.

Recognizing that these simple conditions benchmarks may not be appropriate for more complex conditions, McNally analyzed multiple annual runs that included complex terrain conditions and suggested an alternative set of benchmarks for temperature under more complex conditions.[17] As part of the WRAP meteorological modeling of the western U.S., including the Rocky Mountain Region, as well as for complex terrain in Alaska, Kemball-Cook (2005b[18]) also came up with meteorological model performance benchmarks for complex conditions.

The objective of comparing the 2022 WRF model performance to the benchmarks is to understand how well the model performs relative to other retrospective WRF applications for the U.S. These benchmarks include bias and error benchmarks for temperature, wind direction and mixing ratio as well as the wind speed bias and Root Mean Squared Error (RMSE) between the models and databases. Table 5-1 lists the performance benchmarks for simple and complex conditions against which we will evaluate the WRF results from this study.

Table 5-1. Meteorological model performance benchmarks for simple and complex conditions

Parameter	Simple	Complex
Temperature Bias	≤ ±0.5 K	≤ ±2.0 K
Temperature Error	≤ 2.0 K	≤ 3.5 K
Mixing Ratio Bias	≤ ±1.0 g/kg	NA

[17] McNally, D. E., 2009. "12km MM5 Performance Goals." Presentation to the Ad-Hoc Meteorology Group. 25-June. http://www.epa.gov/scram001/adhoc/mcnally2009.pdf
[18] Kemball-Cook, S., Y. Jia, C. Emery and R. Morris. 2005. "Alaska MM5 Modeling for the 2002 Annual Period to Support Visibility Modeling" Prepared for Western Regional Air Partnership (WRAP). Prepared by Environ International Corporation. September. http://pah.cert.ucr.edu/aqm/308/docs/alaska/Alaska_MM5_DraftReport_Sept05.pdf

Mixing Ratio Error	≤ 2.0 g/kg	NA
Wind Speed Bias	≤ ±0.5 m/s	≤ ±1.5 m/s
Wind Speed RMSE	≤ 2.0 m/s	≤ 2.5 m/s
Wind Direction Bias	≤ ±10 degrees	NA
Wind Direction Error	≤ 30 degrees	≤ 55 degrees

The equations for bias, error, and root mean square error (RMSE) are given below.

Mean Bias (Bias) = $\frac{1}{N}\sum_{i=1}^{N}\left(P_i - O_i\right)$

Mean Absolute Gross Error (Error) = $\frac{1}{N}\sum_{i=1}^{N}\left|P_i - O_i\right|$

Root Mean Square Error (RMSE) = $\left[\frac{1}{N}\sum_{i=1}^{N}\left(P_i - O_i\right)^2\right]^{1/2}$

Figure 5-1 displays an example model performance soccer plot graphic from the LADCO 2016 WRF run. The soccer plots show the bias (x-axis) versus error (y-axis) with the simple and complex performance benchmarks[19] represented by the rectangles. When the WRF monthly performance achieves the benchmark, the symbol for each meteorology variable falls within the central rectangle. In this example we see the 2016 WRF simulation for the test period achieved the complex benchmark for all variables but wind direction.

[19] Note that Figure 5-1 is using the McNally (2009) versions of the complex benchmark for temperature whereas we have adopted the Emory et. al (2001) versions for the temperature and wind benchmarks.

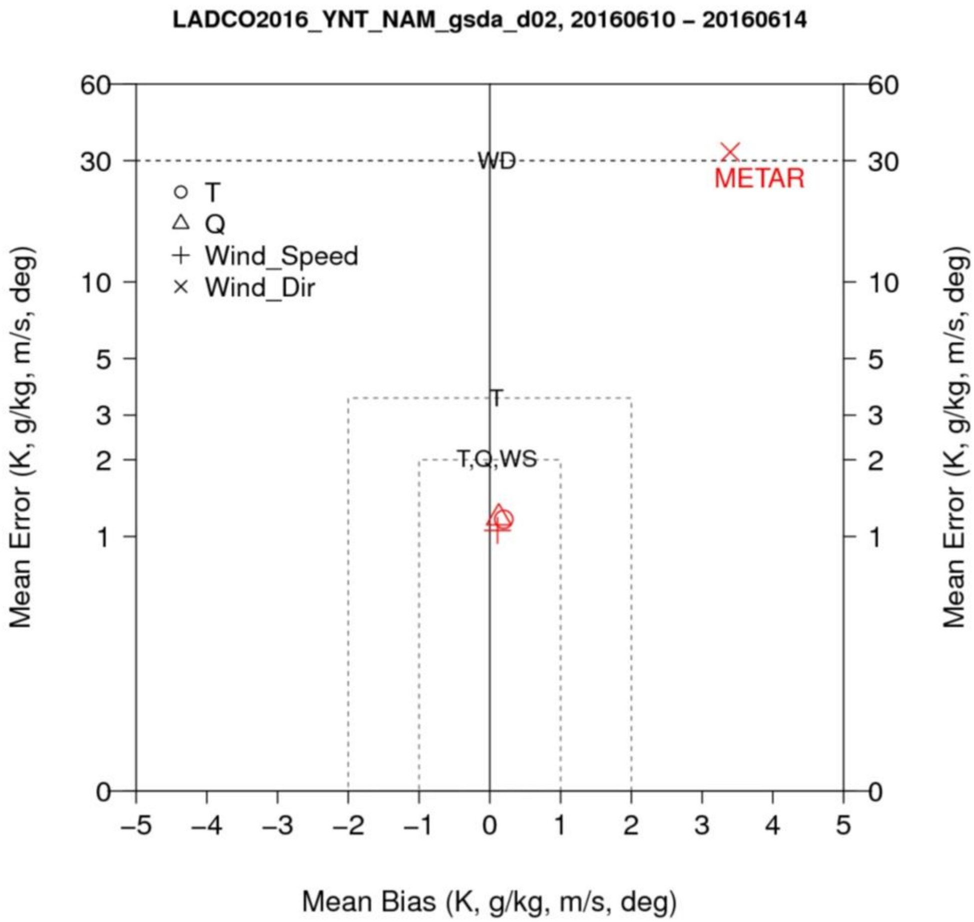

Figure 5-1. Example quantitative model performance evaluation display using a soccer plot to display the model performance for several key variables on a single plot.

5.2 QUANTITATIVE EVALUATION USING UPPER LAYER METEOROLOGICAL OBSERVATIONS

AMET will be used to compare WRF predictions to upper layer observations of winds, temperature, and humidity. Data from the NOAA Wind profiler network will be used to evaluate the u and v wind components from the surface to the tropopause.[20] Upper air profile data from the RAwindonse OBservations (RAOB) network, which includes approximately 100 measurement sites in North America, will be used to evaluate potential

[20] http://www.profiler.noaa.gov/npn/aboutNpnProfilers.jsp

temperature, relative humidity, and the wind components from the surface to the tropopause.

5.3 QUALITATIVE MODEL PERFORMANCE EVALUATION

One of the qualitative model performance evaluations of the 2022 WRF simulation is to compare spatial maps of WRF estimated precipitation with precipitation maps based on observations from NCEP and PRISM. One caveat of this analysis is that the PRISM analysis covers only the Continental U.S. and does not extend offshore or into Canada or Mexico.

Figure 5-2 displays example precipitation comparisons of WRF and PRISM fields from 2011 WRF simulations for the months of January and July and the continental U.S. For the LADCO 2022 WRF modeling, we will compare the model with PRISM for all months, for the 4-km and 1.33-km domains.

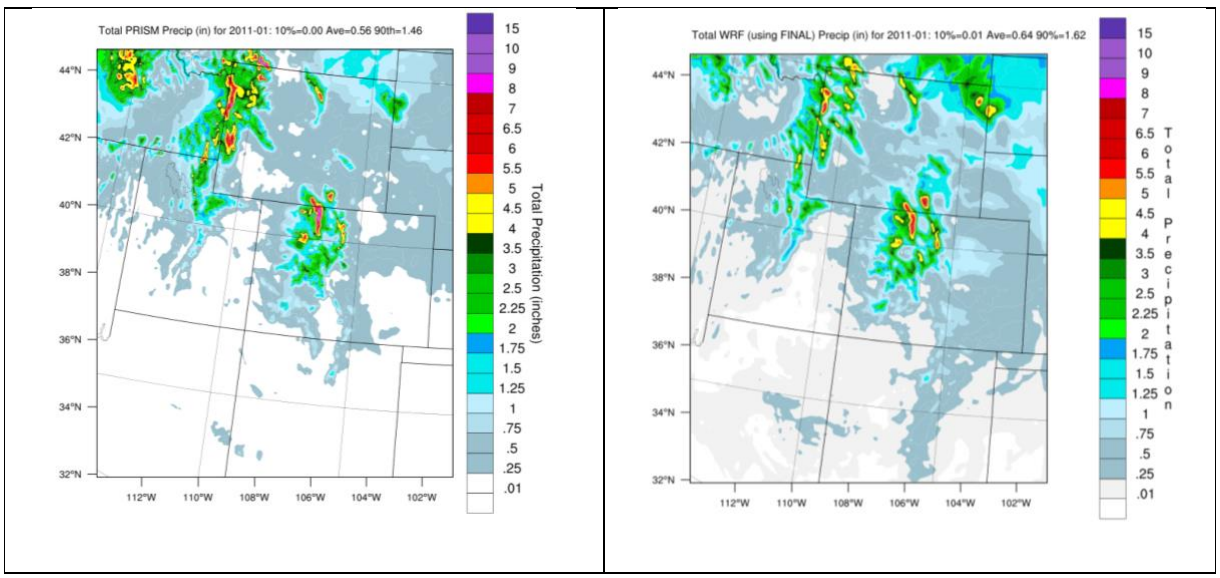

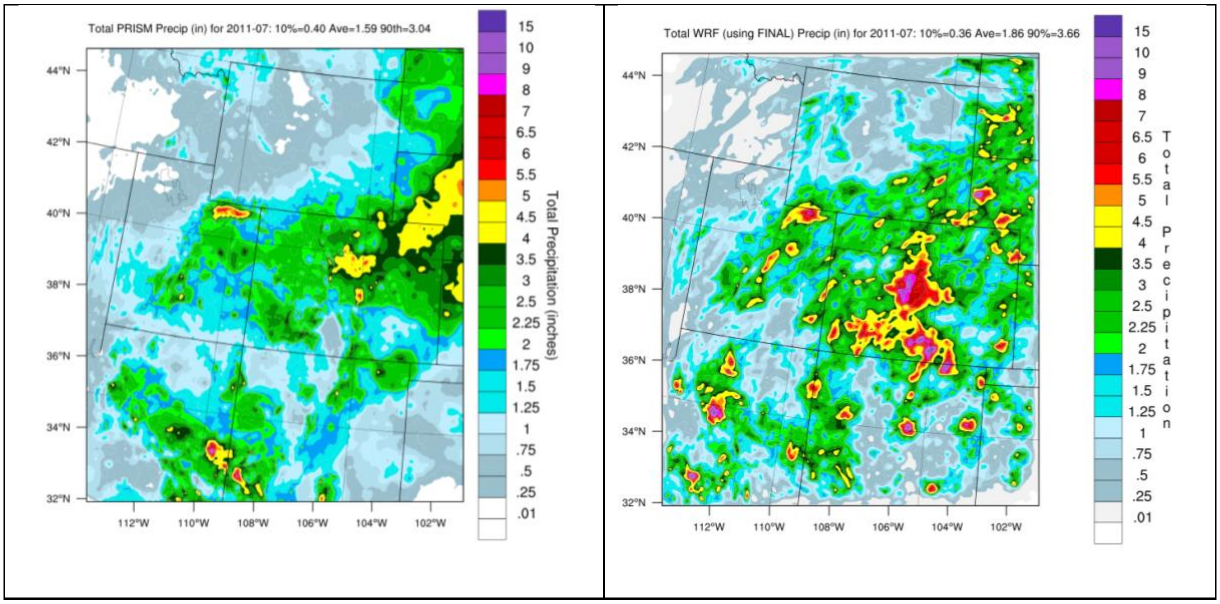

Figure 5-2. Example comparison of PRISM analysis (left) and WRF modeling (right) monthly total precipitation amounts across the a 4km WRF domain for the months of January (top) and July (bottom) from a Western U.S. 2011 WRF simulation

Another qualitative model performance evaluation is to compare model- and observation-based surface weather maps for high ozone and particulate matter episodes to determine whether the synoptic scale feathers are adequately simulated by the model. The National Centers for Environmental Prediction (NCEP), Hydrometeorological Prediction Center, National Weather Service[21] provides observation-based surface weather maps. An example of the NCEP and WRF surface weather maps show in Figure 5-3 will indicate if the model can reproduce the extent and location of the high and low pressure systems, cold fronts, trough lines, and precipitation in the contiguous U.S.

[21] https://www.wpc.ncep.noaa.gov/dailywxmap/explaination.html

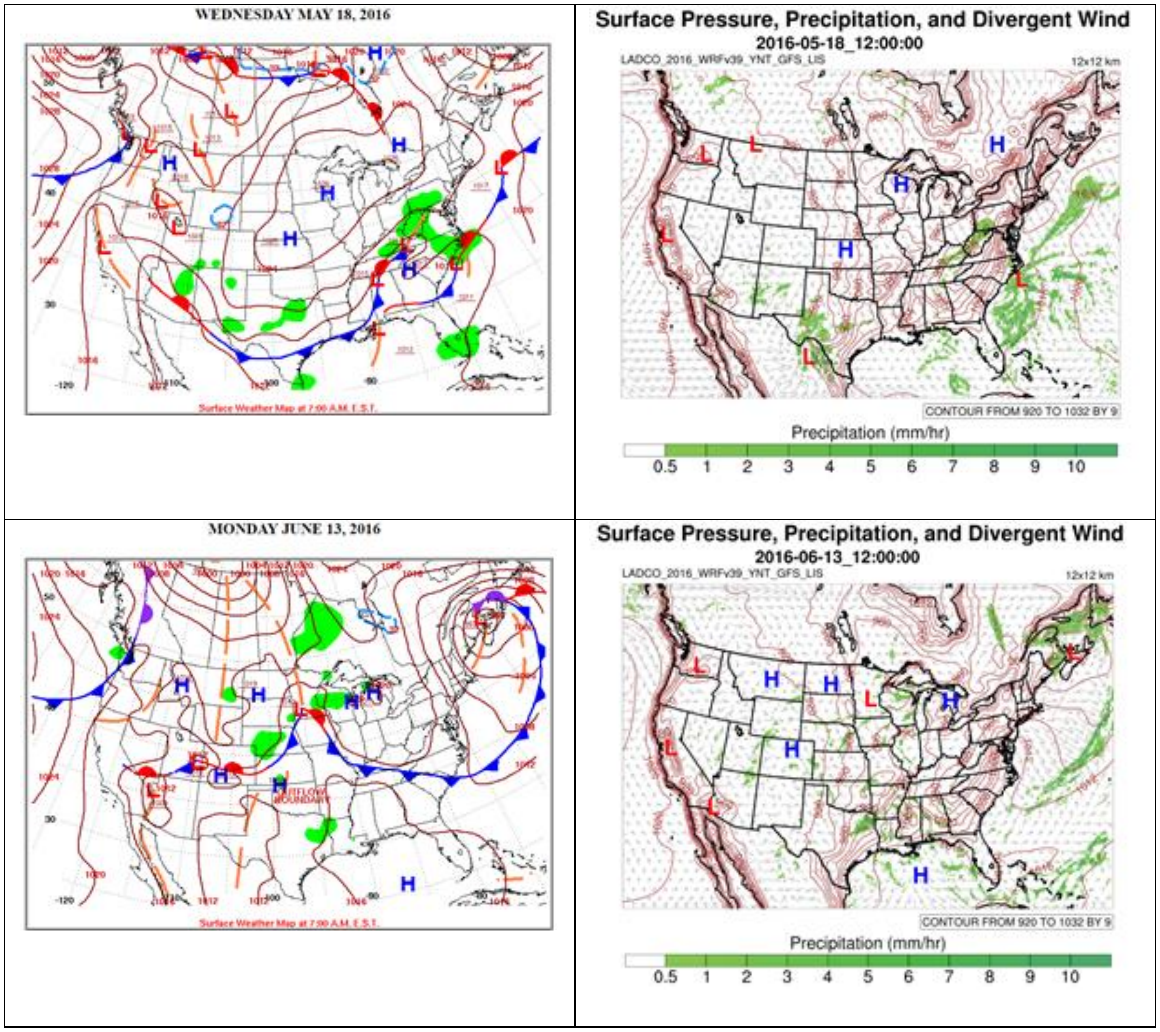

Figure 5-3. Example comparison of surface observation-based (left) and WRF model-based (right) weather maps at 7:00 am EST with modeled outputs at 12:00 pm UTC for May 18, 2016 (top) and June 13, 2016 (bottom)

The model performance evaluation of the 2022 WRF simulation will also compare surface winds of WRF estimated with observations based on the dataset obtained from MADIS during the summer of 2022. The surface wind plots during summer days of 2022 will be used to evaluate whether the WRF model can reproduce the wind convergence zones accompanying the lake breeze frontal movements along the coast of Lake Michigan.

Figure 5-4 shows an example comparison of observed surface winds and results from a WI DNR WRF version 3.8 model simulation for 2011. This plot illustrates that the model had successfully reproduced the surface flow convergence zone associated with the lake breeze that formed on June 4th, 2011 at 4:00pm CDT over Southeastern Wisconsin along the Lake Michigan shoreline.

These plots will be used to evaluate whether WRF can simulate key dynamical features that contribute to high summer ozone along the shores of Lake Michigan.

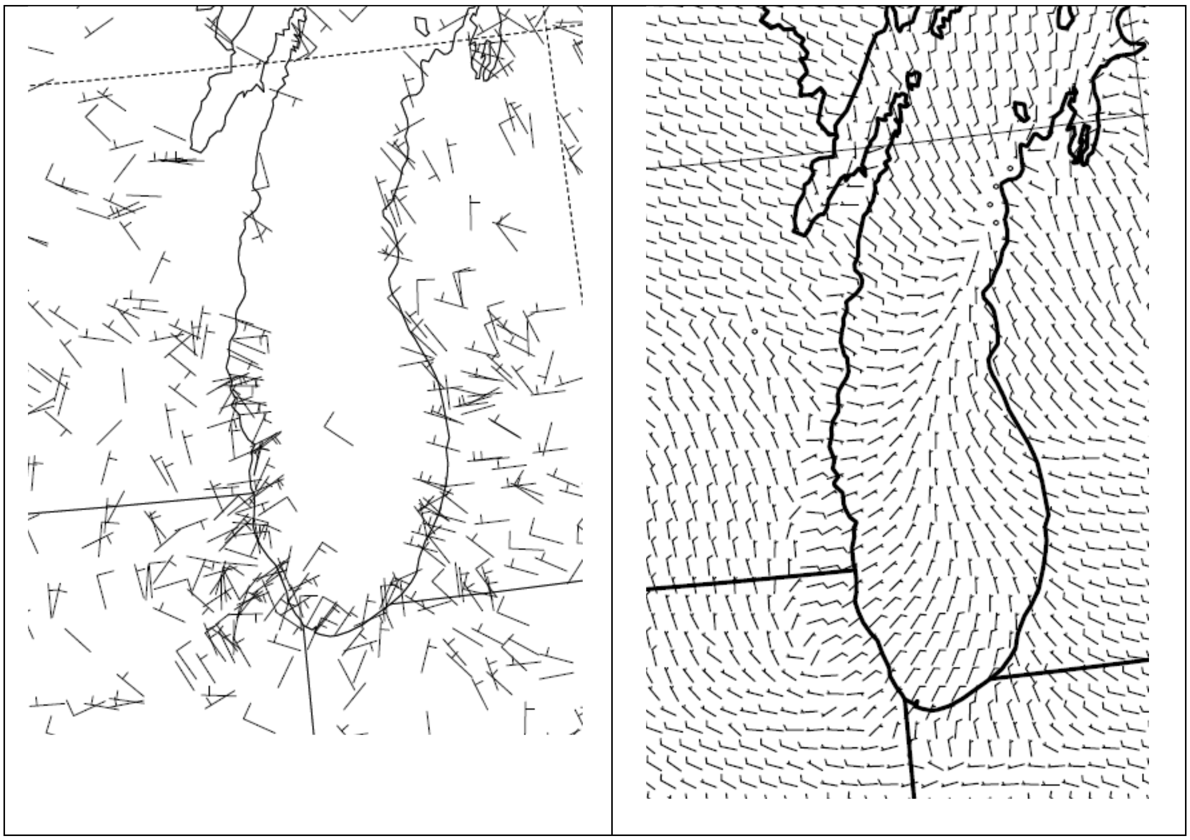

Figure 5-4. Example comparison of observed surface winds (left) and WRF modeling (right) on June 4th, 2011 at 4:00pm CDT from previous WRF model simulations in Wisconsin

Appendix A. LADCO WPS and WRF configuration options for 2022 experiments

WRF Treatment	namelist Variable	WRF39_YNT_GFS6_OBS	WRF45_APX_ERA6_OBS	WRF45_APX_NAM6_OBS	WRF45_YNT_NAM6_OBS	WRF45_APX_NAM_HRRR3	WRF45_YNT_NAM_HRRR3	WRF45_APX_NAM_HRRR3_OBS	WRF45_YNT_NAM_HRRR6	WRF45_APX_NAM_HRRR6_OBS	WRF45_YNT_NAM_HRRR6_OBS
WRF Version		3.9.1	4.5	4.5	4.5	4.5	4.5	4.5	4.5	4.5	4.5
Domain(s)		d01(CONUS),d02 (Midwest and Northeast), d03 (Lake Michigan)	d01(CONUS),d02 (Midwest and Northeast), d03 (Lake Michigan)	d01(CONUS), d02 (Midwest and Northeast), d03 (Lake Michigan)	d01(CONUS), d02 (Midwest and Northeast), d03 (Lake Michigan)	d01(CONUS), d02 (Midwest and Northeast), d03 (Lake Michigan)	d01(CONUS), d02 (Midwest and Northeast), d03 (Lake Michigan)	d01(CONUS),d02 (Midwest and Northeast), d03 (Lake Michigan)	d01(CONUS), d02 (Midwest and Northeast), d03 (Lake Michigan)	d01(CONUS),d02 (Midwest and Northeast), d03 (Lake Michigan)	d01(CONUS),d02 (Midwest and Northeast), d03 (Lake Michigan)
Vertical Diffusion	km_opt	Horizontal Smagorinsky first-order closure (4)	Horizontal Smagorinsky first-order closure (4)	Horizontal Smagorinsky first-order closure (4)	Horizontal Smagorinsky first-order closure (4)	Horizontal Smagorinsky first-order closure (4)	Horizontal Smagorinsky first-order closure (4)	Horizontal Smagorinsky first-order closure (4)	Horizontal Smagorinsky first-order closure (4)	Horizontal Smagorinsky first-order closure (4)	Horizontal Smagorinsky first-order closure (4)
6th order diffusion	diff_6th_opt	6th order numerical diffision, but prohibit up-gradient (2)	6th order numerical diffision, but prohibit up-gradient (2)	6th order numerical diffision, but prohibit up-gradient (2)	6th order numerical diffision, but prohibit up-gradient (2)	6th order numerical diffision, but prohibit up-gradient (2)	6th order numerical diffision, but prohibit up-gradient (2)	6th order numerical diffision, but prohibit up-gradient (2)	6th order numerical diffision, but prohibit up-gradient (2)	6th order numerical diffision, but prohibit up-gradient (2)	6th order numerical diffision, but prohibit up-gradient (2)
Microphysics	mp_physics	Thompson scheme (8)	Morrison 2 moments (10)	Morrison 2 moments (10)	Thompson scheme (8)	Morrison 2 moments (10)	Thompson scheme (8)	Morrison 2 moments (10)	Thompson scheme (8)	Morrison 2 moments (10)	Morrison 2 moments (10)
LW Radiation	ra_lw_physics	RRTMG (4)	RRTMG (4)	RRTMG (4)	RRTMG (4)	RRTMG (4)	RRTMG (4)	RRTMG (4)	RRTMG (4)	RRTMG (4)	RRTMG (4)
SW Radiation	ra_sw_physics	RRTMG (4)	RRTMG (4)	RRTMG (4)	RRTMG (4)	RRTMG (4)	RRTMG (4)	RRTMG (4)	RRTMG (4)	RRTMG (4)	RRTMG (4)

LSM	sf_sfclay_physics sf_surface_physics	MM5 Monin-Obukhov scheme (1) Unified Noah LSM (2)	Pleim-Xiu surface layer option (7) Pleim-Xiu LSM (7)	Pleim-Xiu surface layer option (7) Pleim-Xiu LSM (7)	MM5 Monin-Obukhov scheme (1) Unified Noah LSM (2)	Pleim-Xiu surface layer option (7) Pleim-Xiu LSM (7)	MM5 Monin-Obukhov scheme (1) Unified Noah LSM (2)	Pleim-Xiu surface layer option (7) Pleim-Xiu LSM (7)	MM5 Monin-Obukhov scheme (1) Unified Noah LSM (2)	Pleim-Xiu surface layer option (7) Pleim-Xiu LSM (7)	MM5 Monin-Obukhov scheme (1) Unified Noah LSM (2)
PBL Scheme	bl_pbl_physics	YSU scheme (1)	ACM2 (7)	ACM2 (7)	YSU scheme (1)	ACM2 (7)	YSU scheme (1)	ACM2 (7)	YSU scheme (1)	ACM2 (7)	YSU scheme (1)
Cumulus parameterization	cu_physics	Kain-Fritsch in the 12-km and 4-km domains (1). None in the 1.3-km domain (0).	Kain-Fritsch in the 12-km and 4-km domains (1). None in the 1.3-km domain (0).	Kain-Fritsch in the 12-km and 4-km domains (1). None in the 1.3-km domain (0).	Kain-Fritsch in the 12-km and 4-km domains (1). None in the 1.3-km domain (0).	Kain-Fritsch in the 12-km and 4-km domains (1). None in the 1.3-km domain (0).	Kain-Fritsch in the 12-km and 4-km domains (1). None in the 1.3-km domain (0).	Kain-Fritsch in the 12-km and 4-km domains (1). None in the 1.3-km domain (0).	Kain-Fritsch in the 12-km and 4-km domains (1). None in the 1.3-km domain (0).	Kain-Fritsch in the 12-km and 4-km domains (1). None in the 1.3-km domain (0).	Kain-Fritsch in the 12-km and 4-km domains (1). None in the 1.3-km domain (0).
Initialization Dataset (ICBC)		0.25 GFS Grid4 (~25-km), 6-hr interval	~31-km ECMWF ERA5, 6-hr interval	NAM218 (12-km), 6-hr interval	NAM218 (12-km), 6-hr interval	Blend of NAM218 (12-km) and HRRRv4 (3-km), 3-hr interval	Blend of NAM218 (12-km) and HRRRv4 (3-km), 3-hr interval	Blend of NAM218 (12-km) and HRRRv4 (3-km), 3-hr interval	Blend of NAM218 (12-km) and HRRRv4 (3-km), 6-hr interval	Blend of NAM218 (12-km) and HRRRv4 (3-km), 6-hr interval	Blend of NAM218 (12-km) and HRRRv4 (3-km), 6-hr interval
Analysis nudging	grid_fdda	Yes	Yes	Yes	Yes	Yes	Yes	Yes	Yes	Yes	Yes
Analysis Nudging Coefficients		grid_fdda = 1, 1, 1, guv: 0.0003 (d01), 0.0001 (d02), 0.0000 (d03) gt: 0.0003 (d01), 0.0001(d02), 0.0000	grid_fdda = 1, 1, 0, guv: 0.0003 (d01), 0.0001 (d02), 0.0000 (d03) gt: 0.0003 (d01), 0.0001(d02), 0.0000 (d03) gq: 0.00001	grid_fdda = 1, 1, 0, guv: 0.0003 (d01), 0.0001 (d02), 0.0000 (d03) gt: 0.0003 (d01), 0.0001(d02), 0.0000 (d03) gq: 0.00001 (d01),	grid_fdda = 1, 1, 0, guv: 0.0003 (d01), 0.0001 (d02), 0.0000 (d03) gt: 0.0003 (d01), 0.0001(d02), 0.0000 (d03) gq: 0.00001 (d01),	grid_fdda = 1, 1, 1, guv: 0.0001 (d01), 0.0001 (d02), 0.0001 (d03) gt: 0.0001 (d01), 0.0001(d02), 0.0001 (d03) gq: 0.00001 (d01),	grid_fdda = 1, 1, 1, guv: 0.0001 (d01), 0.0001 (d02), 0.0001 (d03) gt: 0.0001 (d01), 0.0001(d02), 0.0001 (d03) gq: 0.00001 (d01),	grid_fdda = 1, 1, 0, guv: 0.0003 (d01), 0.0001 (d02), 0.0000 (d03) gt: 0.0003 (d01), 0.0001(d02), 0.0000 (d03) gq: 0.00001 (d01),	grid_fdda = 1, 1, 1, guv: 0.0001 (d01), 0.0001 (d02), 0.0001 (d03) gt: 0.0001 (d01), 0.0001(d02), 0.0001 (d03) gq: 0.00001 (d01),	grid_fdda = 1, 1, 0, guv: 0.0003 (d01), 0.0001 (d02), 0.0000 (d03) gt: 0.0003 (d01), 0.0001(d02), 0.0000 (d03) gq: 0.00001 (d01),	grid_fdda = 1, 1, 0, guv: 0.0003 (d01), 0.0001 (d02), 0.0000 (d03) gt: 0.0003 (d01), 0.0001(d02), 0.0000 (d03) gq: 0.00001 (d01),

		(d03) gq: 0.00001 (d01), 0.00001(d02), 0.0000 (d03)	(d01), 0.00001(d02), 0.0000 (d03)	0.00001(d02), 0.0000 (d03)	0.00001(d02), 0.0000 (d03)	0.00001(d02), 0.0001 (d03)	0.00001(d02), 0.0001 (d03)	0.00001(d02), 0.0000 (d03)	0.00001(d02), 0.0001 (d03)	0.00001(d02), 0.0000 (d03)	0.00001(d02), 0.0000 (d03)
PBL Analysis Nudging	if_no_pbl_nudging	None if_no_pbl_nudging_uv = 1, 1, 1, if_no_pbl_nudging_t = 1, 1, 1, if_no_pbl_nudging_q = 1, 1, 1,	None if_no_pbl_nudging_uv = 1, 1, 1, if_no_pbl_nudging_t = 1, 1, 1, if_no_pbl_nudging_q = 1, 1, 1,	None if_no_pbl_nudging_uv = 1, 1, 1, if_no_pbl_nudging_t = 1, 1, 1, if_no_pbl_nudging_q = 1, 1, 1,	None if_no_pbl_nudging_uv = 1, 1, 1, if_no_pbl_nudging_t = 1, 1, 1, if_no_pbl_nudging_q = 1, 1, 1,	None if_no_pbl_nudging_uv = 1, 1, 1, if_no_pbl_nudging_t = 1, 1, 1, if_no_pbl_nudging_q = 1, 1, 1,	None if_no_pbl_nudging_uv = 1, 1, 1, if_no_pbl_nudging_t = 1, 1, 1, if_no_pbl_nudging_q = 1, 1, 1,	None if_no_pbl_nudging_uv = 1, 1, 1, if_no_pbl_nudging_t = 1, 1, 1, if_no_pbl_nudging_q = 1, 1, 1,	None if_no_pbl_nudging_uv = 1, 1, 1, if_no_pbl_nudging_t = 1, 1, 1, if_no_pbl_nudging_q = 1, 1, 1,	None if_no_pbl_nudging_uv = 1, 1, 1, if_no_pbl_nudging_t = 1, 1, 1, if_no_pbl_nudging_q = 1, 1, 1,	None if_no_pbl_nudging_uv = 1, 1, 1, if_no_pbl_nudging_t = 1, 1, 1, if_no_pbl_nudging_q = 1, 1, 1,
OBSGRID Inputs		LDAD mesonet, METAR, RAOB,Profiler	RDA surface	RDA surface	RDA surface	None	None	RDA surface	None	RDA surface	RDA surface
Obs_grid Nudging	grid_gfdda	Yes	No	Yes	Yes	No (effectively)	No (effectively)	Yes	No (effectively)	Yes	Yes
Obs Nudging Coefficients		grid_sfdda = 1, 1, 1, guv_sfc: 0.0003 (d01), 0.0001 (d02), 0.000 (d03) gt_sfc: 0.0003 (d01), 0.0001 (d02), 0.000 (d03)	grid_sfdda = 1, 1, 0, guv_sfc: 0.0003 (d01), 0.0001 (d02), 0.000 (d03) gt_sfc: 0.0003 (d01), 0.0001 (d02), 0.000 (d03)	grid_sfdda = 1, 1, 0, guv_sfc: 0.0003 (d01), 0.0001 (d02), 0.000 (d03) gt_sfc: 0.0003 (d01), 0.0001 (d02), 0.000 (d03) gq_sfc: 0.0001 (d01), 0.0001 (d02), 0.000 (d03)	grid_sfdda = 1, 1, 0, guv_sfc: 0.0003 (d01), 0.0001 (d02), 0.000 (d03) gt_sfc: 0.0003 (d01), 0.0001 (d02), 0.000 (d03) gq_sfc: 0.0001 (d01), 0.0001 (d02), 0.000 (d03)	grid_sfdda = 1, 1, 1, guv_sfc: 0.000 (d01), 0.000 (d02), 0.000 (d03) gt_sfc: 0.000 (d01), 0.000 (d02), 0.000 (d03) gq_sfc: 0.000 (d01), 0.000 (d02), 0.000 (d03)	grid_sfdda = 1, 1, 1, guv_sfc: 0.000 (d01), 0.000 (d02), 0.000 (d03) gt_sfc: 0.000 (d01), 0.000 (d02), 0.000 (d03) gq_sfc: 0.000 (d01), 0.000 (d02), 0.000 (d03)	grid_sfdda = 1, 1, 0, guv_sfc: 0.0003 (d01), 0.0001 (d02), 0.000 (d03) gt_sfc: 0.0003 (d01), 0.0001 (d02), 0.000 (d03) gq_sfc: 0.0001 (d01), 0.0001 (d02), 0.000 (d03)	grid_sfdda = 1, 1, 1, guv_sfc: 0.000 (d01), 0.000 (d02), 0.000 (d03) gt_sfc: 0.000 (d01), 0.000 (d02), 0.000 (d03) gq_sfc: 0.000 (d01), 0.000 (d02), 0.000 (d03)	grid_sfdda = 1, 1, 0, guv_sfc: 0.0003 (d01), 0.0001 (d02), 0.000 (d03) gt_sfc: 0.0003 (d01), 0.0001 (d02), 0.000 (d03) gq_sfc: 0.0001 (d01), 0.0001 (d02), 0.000 (d03)	grid_sfdda = 1, 1, 0, guv_sfc: 0.0003 (d01), 0.0001 (d02), 0.000 (d03) gt_sfc: 0.0003 (d01), 0.0001 (d02), 0.000 (d03) gq_sfc: 0.0001 (d01), 0.0001 (d02), 0.000 (d03)

		gq_sfc: 0.0001 (d01), 0.0001 (d02), 0.000 (d03)	gq_sfc: 0.0001 (d01), 0.0001 (d02), 0.000 (d03)								
Observation Nudging	obs_nudge_opt	None	None	None	None	None	None	None	None	None	None
LULC		NLCD 2011	NLCD 2011	NLCD 2011	NLCD 2011	NLCD 2011	NLCD 2011	NLCD 2011	NLCD 2011	NLCD 2011	NLCD 2011
External Soil data		SpoRT LIS soil T&Q for d02-d04	NA	NA	NA	NA	NA	NA	NA	NA	NA
SST		GLSEA SST (2-km) over the Great Lakes GHRSST (10-km) for other water bodies	Diagnostic SST from ERA5	Diagnostic SST from NAM	Diagnostic SST from NAM	Diagnostic SST from NAM-HRRR	Diagnostic SST from NAM-HRRR	Diagnostic SST from NAM-HRRR	Diagnostic SST from NAM-HRRR	Diagnostic SST from NAM-HRRR	Diagnostic SST from NAM-HRRR

Appendix B. WRF namelist file

Download the LADCO WRF45_APX_NAM_HRRR6_obs namelist

Appendix C. WRF Model Performance Plots

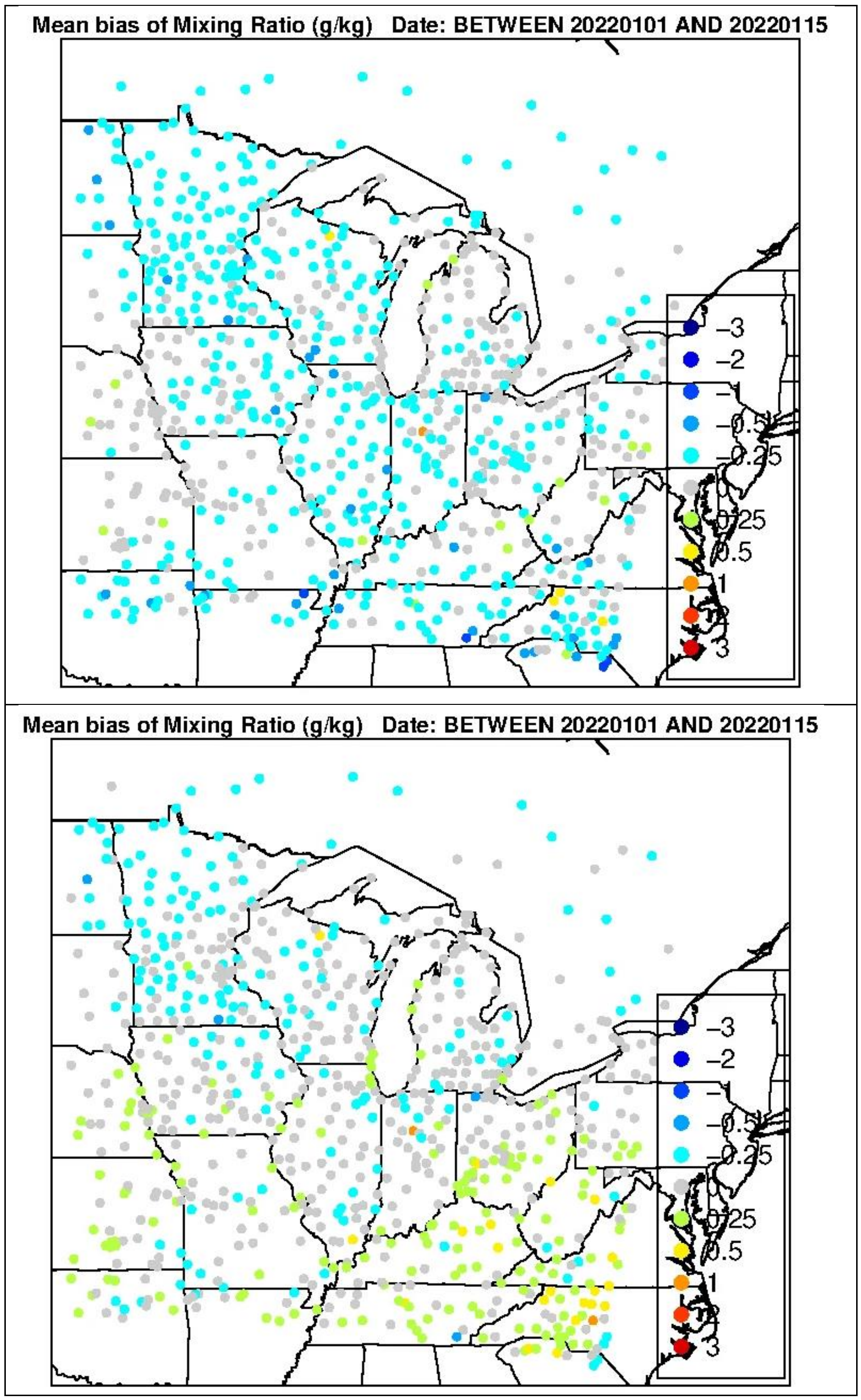

Figure C-1. January 1-15, 2022 average 2-m mixing ratio bias for simulations WRF45_YNT_NAM_HRRR6_obs (top) and WRF45_APX_NAM_HRRR6_obs (bottom)

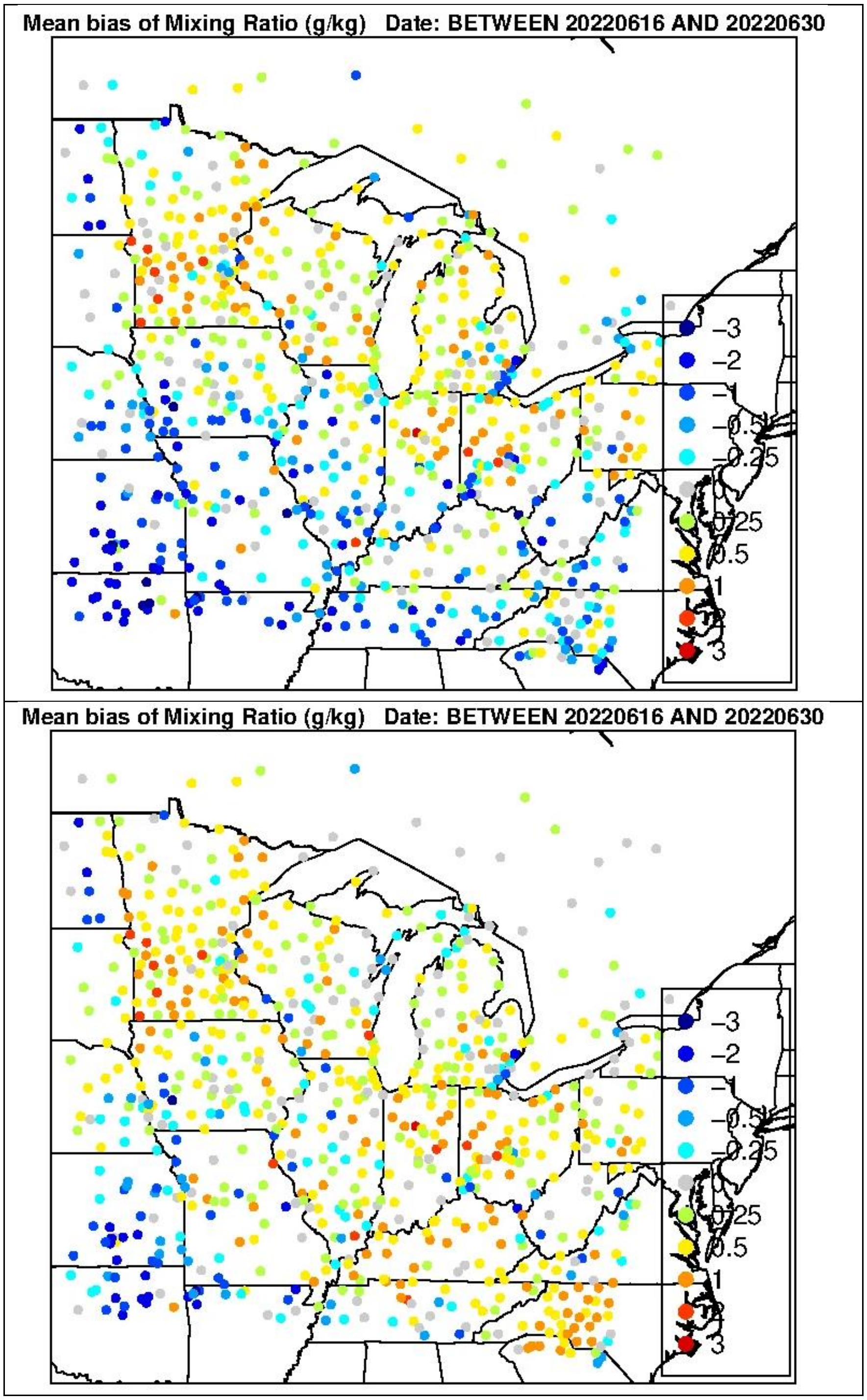

Figure C-2. June 16-30, 2022 average 2-m mixing ratio bias for simulations WRF45_YNT_NAM_HRRR6_obs (top) and WRF45_APX_NAM_HRRR6_obs (bottom)

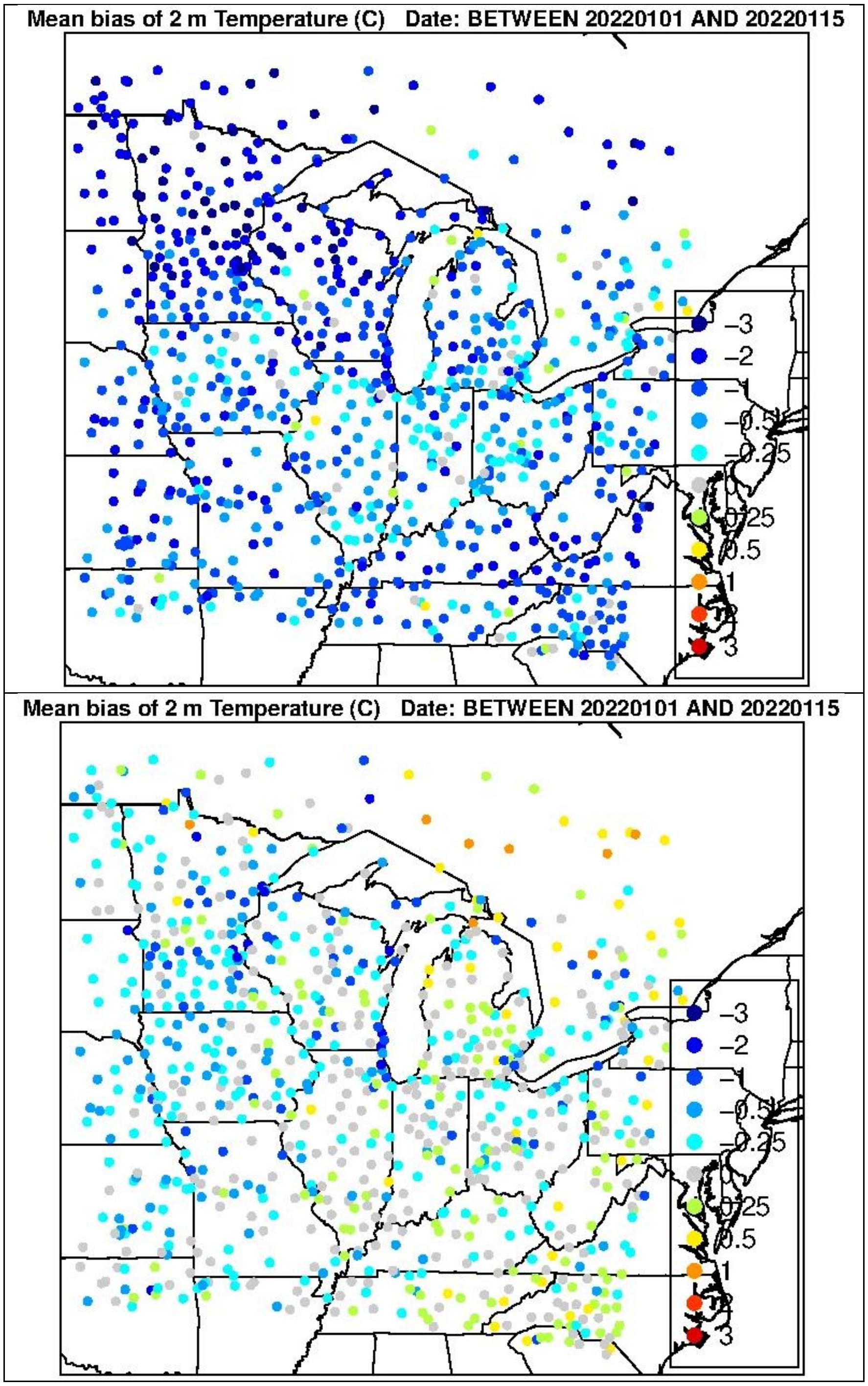

Figure C-3. January 1-15, 2022 average 2-m temperature bias for simulations WRF45_YNT_NAM_HRRR6_obs (top) and WRF45_APX_NAM_HRRR6_obs (bottom)

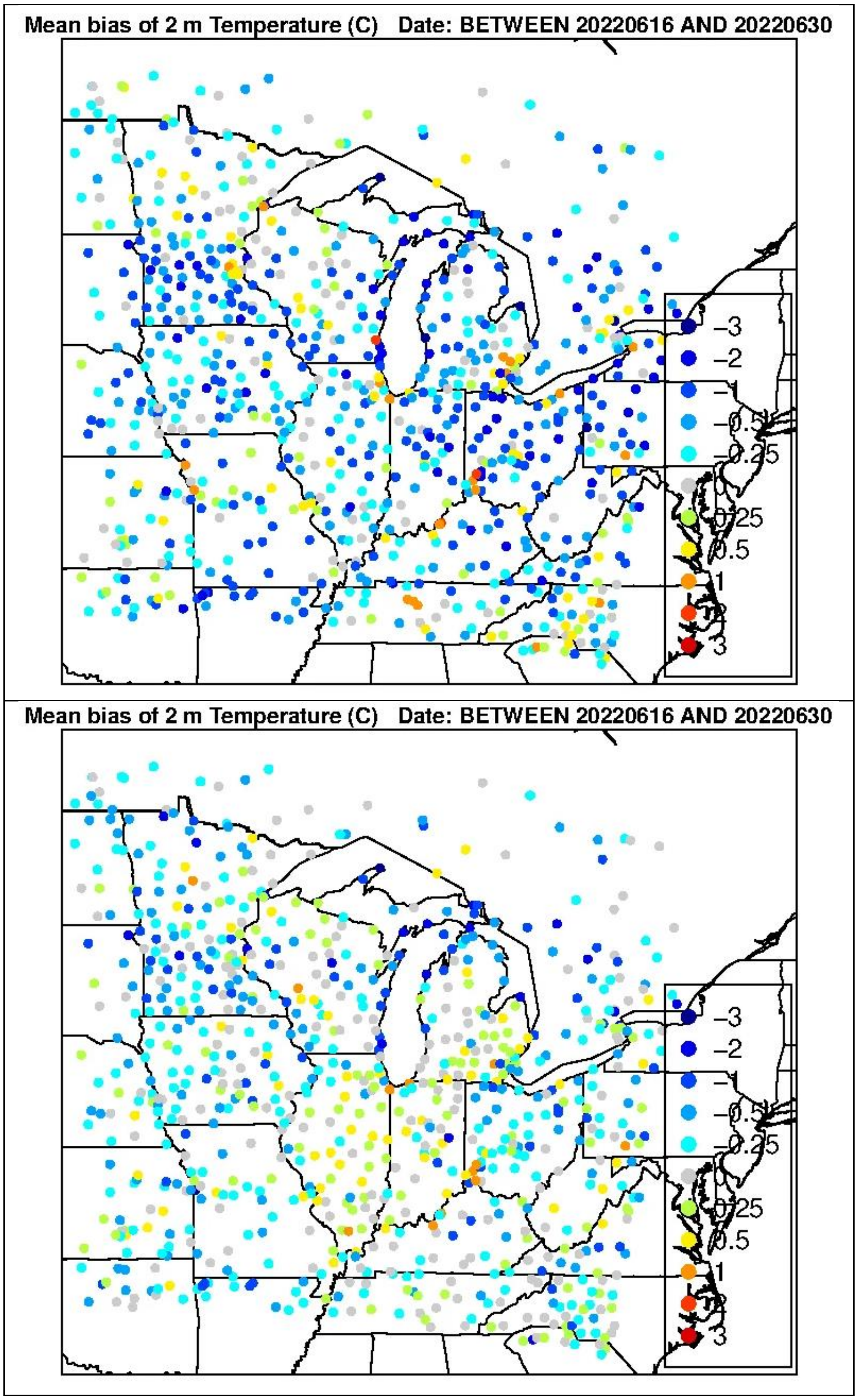

Figure C-4. June 16-30, 2022 average 2-m temperature bias for simulations WRF45_YNT_NAM_HRRR6_obs (top) and WRF45_APX_NAM_HRRR6_obs (bottom)

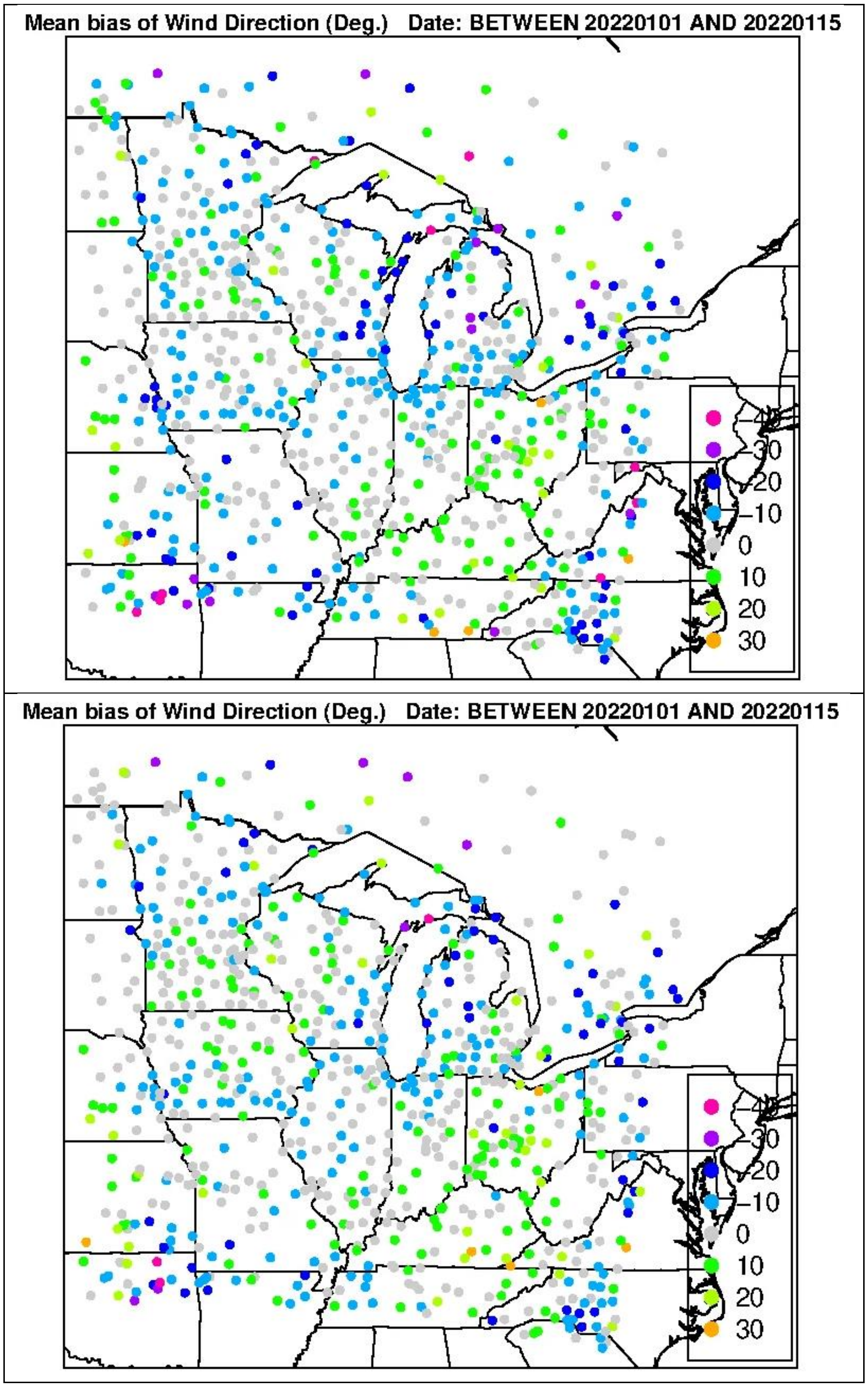

Figure C-5. January 1-15, 2022 average 10-m wind direction bias for simulations WRF45_YNT_NAM_HRRR6_obs (top) and WRF45_APX_NAM_HRRR6_obs (bottom)

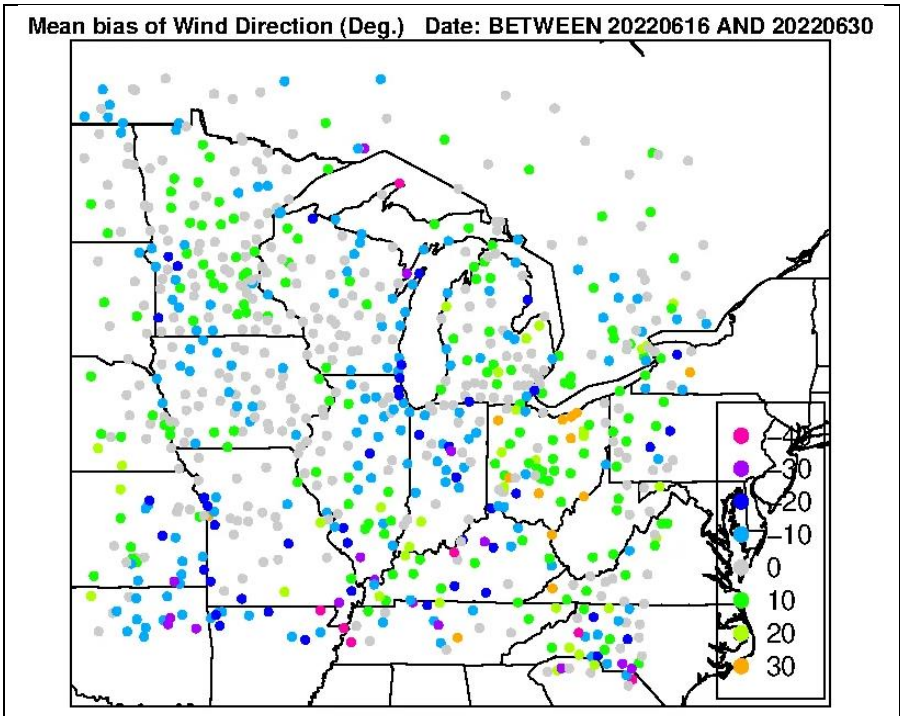

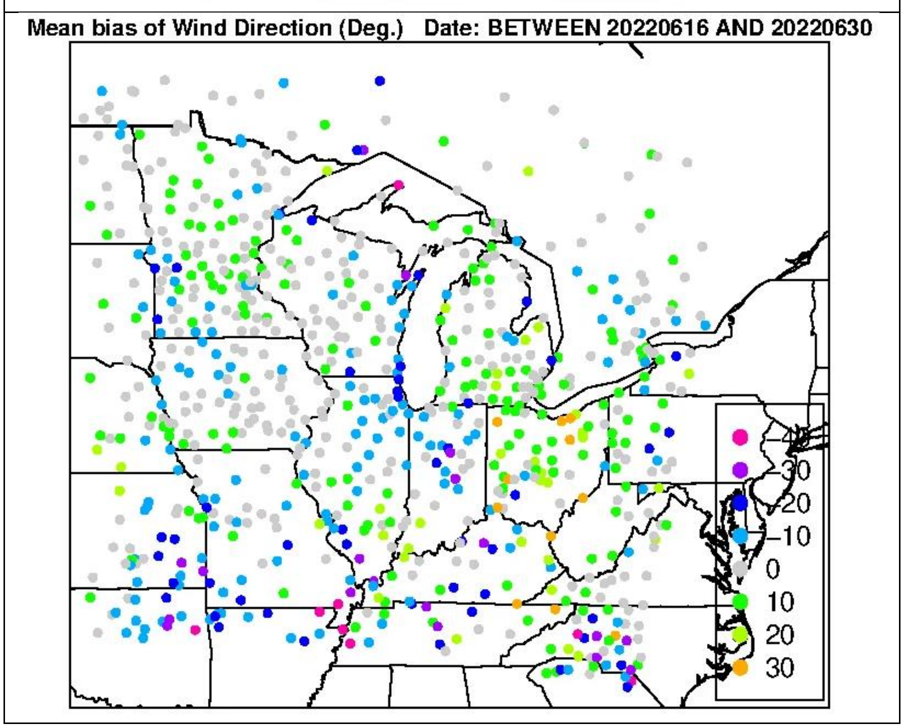

Figure C-6. June 16-30, 2022 average 10-m wind direction bias for simulations WRF45_YNT_NAM_HRRR6_obs (top) and WRF45_APX_NAM_HRRR6_obs (bottom)

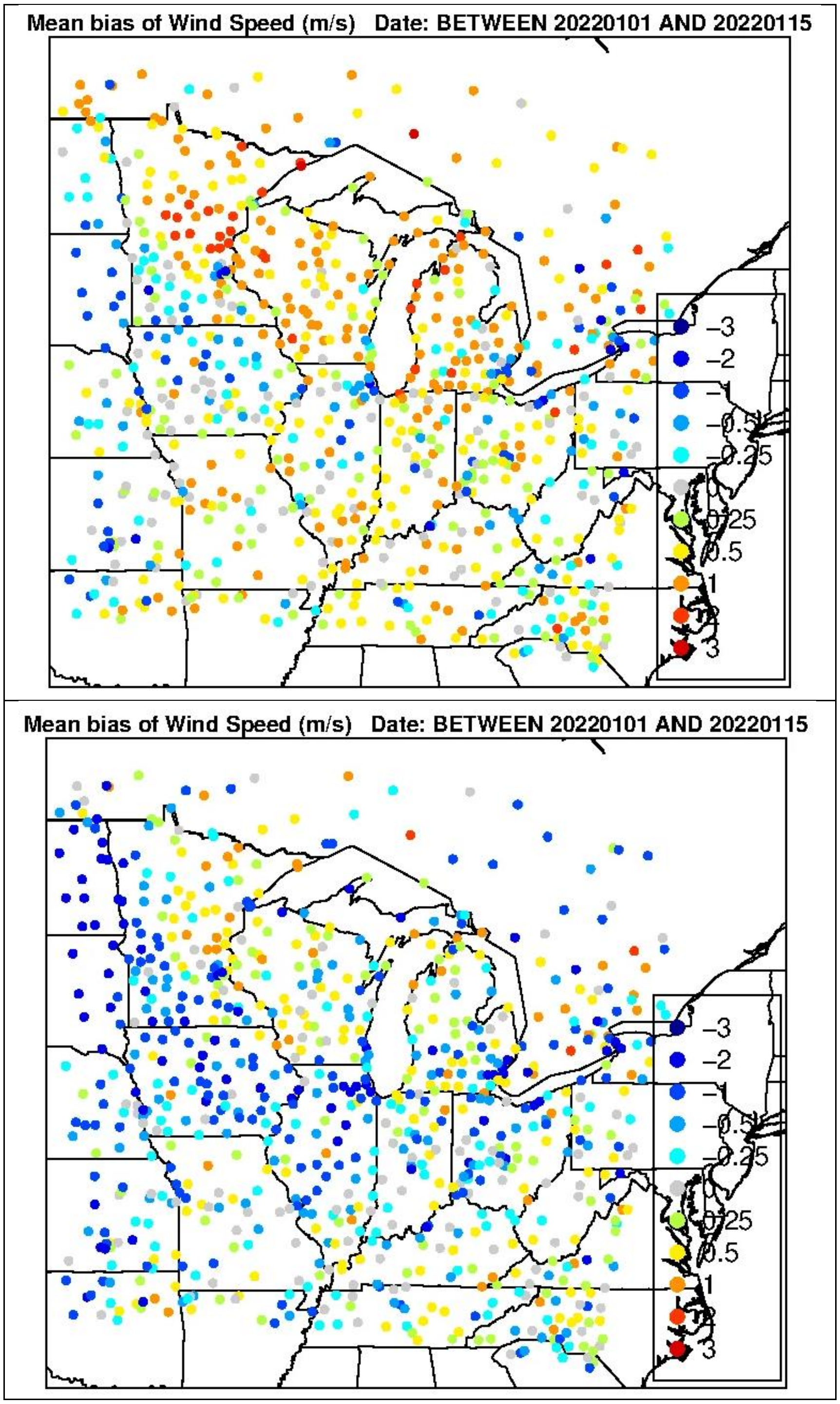

Figure C-7. January 1-15, 2022 average 10-m wind speed bias for simulations WRF45_YNT_NAM_HRRR6_obs (top) and WRF45_APX_NAM_HRRR6_obs (bottom)

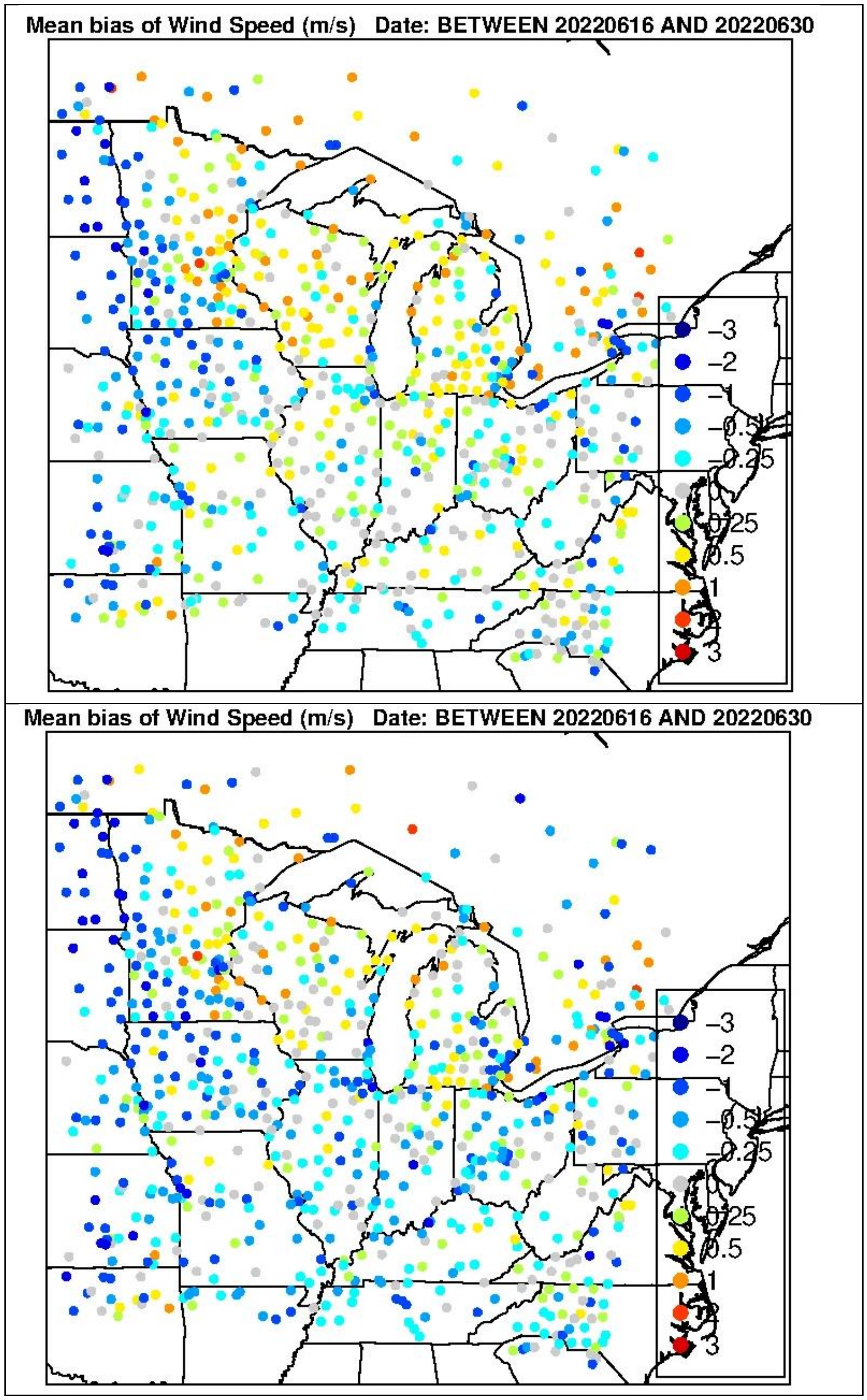

Figure C-8. June 16-30, 2022 average 10-m wind speed bias for simulations WRF45_YNT_NAM_HRRR6_obs (top) and WRF45_APX_NAM_HRRR6_obs (bottom)

6 References

Ashish Sharma, Harindra J.S. Fernando, Alan F. Hamlet, Jessica J. Hellmann, Michael Barlage, Fei Chen, 2016. Urban meteorological modeling using WRF: a sensitivity study, International Journal of Climatology. July 2016. (wileyonlinelibrary.com) DOI: 10.1002/joc.4819.

Brian K. Blaylock, John D. Horel, and Erik T. Crosman, 2017. Impact of Lake Breezes on Summer Ozone Concentrations in the Salt Lake Valley, Journals Online, American Meteorological Society, February 2017. (https://doi.org/10.1175/JAMC-D-16-0216.1

Boylan, J.W., Russell, A.G., 2006. PM and light extinction model performance metrics, goals, and criteria for three-dimensional air quality models. Atmospheric Environment 40, 4946-4959.

Carlton, A.G., Baker, K.R., 2011. Photochemical Modeling of the Ozark Isoprene Volcano: MEGAN, BEIS, and Their Impacts on Air Quality Predictions. Environmental Science & Technology 45, 4438-4445.

Cooper, O.R., Stohl, A., Hubler, G., Hsie, E.Y., Parrish, D.D., Tuck, A.F., Kiladis, G.N., Oltmans, S.J., Johnson, B.J., Shapiro, M., Moody, J.L., Lefohn, A.S., 2005. Direct Transport of Midlatitude Stratospheric Ozone into the Lower Troposphere and Marine Boundary Layer of the Pacific Ocean. Journal of Geophysical Research – Atmospheres 110, D23310, doi:10.1029/2005JD005783.

ENVIRON, 2008. User's Guide Comprehensive Air Quality Model with Extensions. ENVIRON International Corporation, Novato.

Gilliam, R.C., Pleim, J.E., 2010. Performance Assessment of New Land Surface and Planetary Boundary Layer Physics in the WRF-ARW. Journal of Applied Meteorology and Climatology 49, 760-774.

Heath, Nicholas K., Pleim, J.E., Gilliam, R., Kang, D., 2016. A simple lightning assimilation technique for improving retrospective WRF simulations. Journal of Advances in Modeling Earth Systems. 8.10.1002/2016MS000735.

Jin, Suming, Homer, Collin, Yang, Limin, Danielson, Patrick, Dewitz, Jon, Li, Congcong, Zhu, Z., Xian, George, Howard, Danny, Overall methodology design for the United States National Land Cover Database 2016 products: Remote Sensing, v. 11, no. 24, at https://doi.org/10.3390/rs11242971

LADCO, 2022. Weather Research Forecast 2016 Meteorological Model Simulation and Evaluation, LADCO Technical Support Document, June 22, 2022, https://www.ladco.org/wp-content/uploads/Modeling/2016/WRF/LADCO_2016WRF_Performance_22June2022.pdf

Langford, A.O., Reid, S.J., 1998. Dissipation and Mixing of a Small-Scale Stratospheric Intrusion in the Upper Troposphere. Journal of Geophysical Research 103, 31265-31276.

Jason A. Otkin, Lee M. Cronce, Jonathan L. Case, R. Bradley Pierce, Monica Harkey, Allen Lenzen, David S. Henderson, Zac Adelman, Tsengel Nergui, and Christopher R. Hain, 2023. Meteorological modeling sensitivity to parameterizations and satellite-derived surface datasets during the 2017 Lake Michigan Ozone Study, Atmos. Chem. Phys., 23, 7935–7954, https://doi.org/10.5194/acp-23-7935-2023, 2023

Otte, T.L., 2008. The impact of nudging in the meteorological model for retrospective air quality simulations. Part II: Evaluating collocated meteorological and air quality observations. Journal of Applied Meteorology and Climatology, 47(7): 1868-1887.

Otte, T.L., Pleim, J.E., 2010. The Meteorology-Chemistry Interface Processor (MCIP) for the CMAQ modeling system: updates through MCIPv3.4.1. Geoscientific Model Development 3, 243-256.

Skamarock, W.C., Klemp, J.B., Dudhia, J., Gill, D.O., Barker, D.M., Duda, M.G., Huang, X., Wang, W., Powers, J.G., 2008. A Description of the Advanced Research WRF Version 3.

Stammer, D., F.J. Wentz, and C.L. Gentemann, 2003, Validation of Microwave Sea Surface Temperature Measurements for Climate Purposes, J. Climate, 16, 73-87. 114 United States Environmental Protection Agency Office of Air Quality Plan

US EPA, 1991. Guideline on the Regulatory Application of the Urban Airshed Model. U.S. Environmental Protection Agency, Office of Air Quality Planning and Standards, technical Support Division, Source Receptor Analysis Branch, Research Triangle Park, NC.

US EPA, 2018. Modeling Guidance for Demonstrating Attainment of Air Quality Goals for Ozone, PM2.5, and Regional Haze, EPA 454/R-18-009 November 2018, https://www.epa.gov/sites/default/files/2020-10/documents/o3-pm-rh-modeling_guidance-2018.pdf

US EPA, 2019. Meteorological Model Performance for Annual 2016 Simulation WRFv3.8, EPA-454/R-19-010, July 2019, https://www.epa.gov/sites/default/files/2020-10/documents/met_model_performance-2016_wrf.pdf

US EPA, 2022. Meteorological Model Performance for Annual 2017 Simulation WRFv3.8, EPA-454/R-22-006, September 2022, https://www.epa.gov/system/files/documents/2022-09/MET_TSD_2017.pdf

US EPA, 2024. Meteorological Model Performance for Annual 2022 Simulation WRF v4.4.2, EPA-454/R-24-001 March 2024, https://www.epa.gov/system/files/documents/2024-03/wrf_2022_tsd.pdf